

2  
3 **Zygotic Genome Activation Occurs Shortly After Fertilization in**  
4 **Maize**

5  
6 **Junyi Chen<sup>1+</sup>, Nicholas Strieder<sup>2+</sup>, Nadia G. Krohn<sup>1,3</sup>, Philipp Cyprys<sup>1</sup>, Stefanie**  
7 **Sprunck<sup>1</sup>, Julia C. Engelmann<sup>2</sup>, and Thomas Dresselhaus<sup>1\*</sup>**

8  
9 <sup>1</sup>Cell Biology and Plant Biochemistry, Biochemie-Zentrum Regensburg, University of  
10 Regensburg, 93053 Regensburg, Germany.

11 <sup>2</sup>Institute of Functional Genomics, University of Regensburg, 93053 Regensburg, Germany.

12 <sup>3</sup>Present address: Department of Agriculture, Regional Campus of Umuarama, State  
13 University of Maringa, 87507-190, Umuarama, PR, Brazil.

14 \*Corresponding author: thomas.dresselhaus@ur.de

15 +Equal contributors

16  
17 **Short title:** Zygotic gene activation in maize

18  
19 **One-sentence summary:** Transcription profiles generated from maize gametes and zygotes  
20 at different stages reveal a highly dynamic zygotic genome activation pattern, providing  
21 insights into early embryo development.

22  
23 The author responsible for distribution of materials integral to the findings presented in this  
24 article in accordance with the policy described in the Instructions for Authors  
25 (www.plantcell.org) is: Thomas Dresselhaus (thomas.dresselhaus@ur.de)

26  
27  
28 **ABSTRACT**

29 The formation of a zygote via the fusion of an egg and sperm cell and its subsequent  
30 asymmetric division (ACD) herald the start of the plant's life cycle. Zygotic genome activation  
31 (ZGA) is thought to occur gradually, with the initial steps of zygote and embryo development  
32 being primarily maternally controlled, and subsequent steps being governed by the zygotic  
33 genome. Here, using maize (*Zea mays*) as a model plant system, we determined the timing  
34 of zygote development and generated RNA-Seq transcriptome profiles of gametes, zygotes,  
35 and apical and basal daughter cells. ZGA occurs shortly after fertilization and involves about  
36 10% of the genome being activated in a highly dynamic pattern. In particular, genes  
37 encoding transcriptional regulators of various families are activated shortly after fertilization.  
38 Further analyses suggested that chromatin assembly is strongly modified after fertilization,  
39 that the egg cell is primed to activate the translational machinery, and that hormones likely  
40 play a minor role in the initial steps of early embryo development in maize. Our findings  
41 provide important insights into gamete and zygote activity in plants, and our RNA-Seq  
42 transcriptome profiles represent a comprehensive, unique RNA-Seq dataset that can be  
43 used by the research community.

44  
45 **INTRODUCTION**

46 The life cycles of animals and plants begin with the formation of a zygote, containing  
47 the cytoplasm from two gametes, a large egg cell and a small sperm cell. This single  
48 cell then develops via embryogenesis into an entire organism consisting of hundreds  
49 of different cell types. In contrast to most animal systems, the flowering plant zygote

50 divides asymmetrically into daughter cells of completely different cell fates. While the  
51 small, cytoplasm-rich apical daughter cell further develops into the embryo proper,  
52 the highly vacuolated basal cell gives rise to the suspensor, which delivers nutrients  
53 to the embryo and positions the embryo proper in the surrounding endosperm tissue  
54 of the developing seed. Little is known about the establishment of zygote polarity and  
55 the gene regulatory network that leads to asymmetric cell division and cell fate  
56 determination in both daughter cells (Zhao et al., 2017). Due to the unequal  
57 distribution of their cytoplasm, it is generally thought that maternal factors contributed  
58 by the egg regulate zygote and early embryo development. The maternal-to-zygotic  
59 transition (MZT) depends on both zygotic genome activation (ZGA) and the  
60 degradation of maternal components. In animals, ZGA occurs after the first cell cycle  
61 in mammals and as late as the sixth to eighth round of the cell cycle in insects, fish,  
62 and amphibians (Schier, 2007; Lee et al., 2014). The time point at which ZGA occurs  
63 in plants has long been debated. Currently, the zygote is thought to be in a relatively  
64 quiescent transcriptional state, and ZGA is thought to occur gradually rather than as  
65 an all-or-none process initiated before the first division (Baroux and Grossniklaus,  
66 2015; Zhao and Sun, 2015). However, analyses of a few candidate genes have  
67 indicated that ZGA in flowering plants occurs before zygotic division (Zhao et al.,  
68 2017).

69 To characterize the onset of ZGA at the whole-genome level, it is necessary  
70 to determine the transcriptome profiles of both gametes and to identify *de novo*  
71 generated transcripts from the zygotic genome. In the current study, we established  
72 methods to manually isolate living male and female gametes, zygotes at different  
73 stages, and their daughter cells using maize (*Zea mays*) as a model flowering plant.  
74 We then generated RNA-Seq data from these cells and investigated the  
75 transcriptome dynamics after fertilization. We compared the transcriptomes of maize  
76 and *Oryza sativa* (rice) gametes and explored how the cell cycle, chromatin, and  
77 auxin pathways are regulated after fertilization. Finally, we identified transcription  
78 factor (TF) and receptor-like kinase genes associated with the various cell types and  
79 zygotic stages and found that ZGA in maize occurs shortly after fertilization,  
80 displaying a highly dynamic pattern.

81

82

## 83 RESULTS AND DISCUSSION

### 84 Manual cell isolation, RNA-Seq, validation, and data quality

85 Maize plants were grown in indoor walk-in growth rooms to reduce seasonal  
86 variability in zygote development. We manually isolated cells of the inbred line B73  
87 at 2-h intervals over a 2.5-day period as described in Methods. We used DAPI  
88 staining as a gross indicator to investigate cell cycle stages. As shown in **Figure 1A**,  
89 sperm cells consist mainly of the nucleus, containing highly condensed chromatin.  
90 Egg cell chromatin appeared less condensed than sperm cell chromatin and stained  
91 very weakly with DAPI. The strongest DAPI staining was detected in zygotes at 24  
92 hours after pollination (HAP), indicating that S-phase was complete. Early anaphase  
93 occurred at ~30 HAP, and telophase began at 35 HAP. Cytokinesis was visible at 43  
94 HAP, and asymmetric cell division (ACD) was completed by 48 HAP. The small  
95 cytoplasm-rich apical and vacuolated basal cells could be manually separated at ~52  
96 HAP.

97 The protocol used to generate RNA-Seq data from only a few plant cells is  
98 described in Methods. Three biological replicates were prepared from approximately  
99 1,000 sperm cells each and 13–20 cells each for the other stages (**Table 1**, see also  
100 **Supplemental Table 1** and **Supplemental Figures 1 and 2** for samples,  
101 sequencing details, and library quality). A gene expression master list, containing the  
102 median expression values of each cell type for the 39,469 annotated maize genes,  
103 protein annotations, and homologs from *Arabidopsis thaliana* and rice is provided in  
104 **Supplemental Data Set 1**.

105 For validation and initial analysis of the dynamics of gene expression patterns  
106 obtained from the RNA-Seq data, we focused on the transcript levels of 12 genes  
107 that were previously shown (by single-cell RT-PCR) to be highly or differentially  
108 expressed during fertilization and zygote development in maize (Engel et al., 2003).  
109 In agreement with previous results, the gamete-expressed membrane protein genes  
110 *ZmGEX1* (SP vs. all:  $\log_2FC >4.0^*$ ) and *ZmGEX2* (SP vs. all:  $\log_2FC >7.4^*$ ) were  
111 highly and specifically expressed in sperm cells, as were *Zmsp271* (SP vs. all:  
112  $\log_2FC >3.8^*$ ) and *Zmsp041* (SP vs. all:  $\log_2FC >5.2^*$ ), which were identified in the  
113 same screen (**Figure 1I**, **Supplemental Data Sets 1–3**). *ZmEA1* (EC vs. SP:  $\log_2FC$   
114  $=8.7^*$ ) and *ZmES1-4* (EC vs. AC/BC:  $\log_2FC >2.9$  to  $9.7^*$ , Zy24 vs. AC/BC:  $\log_2FC$   
115  $>2.4$  to  $8.7^*$ ), encoding secreted peptides required for micropylar pollen tube

116 guidance and pollen tube burst, respectively, were highly expressed in egg cells and  
117 synergids and were significantly downregulated after fertilization (Cordts et al., 2001;  
118 Marton et al., 2005; Amien et al., 2010) (**Supplemental Data Set 3**). The cell cycle  
119 genes *ZmMCM3*, *ZmMCM6*, *ZmCycB1;2*, and *ZmCycB2;1* were previously shown to  
120 be induced after fertilization (Sauter et al., 1998; Dresselhaus et al., 1999b;  
121 Dresselhaus et al., 2006). Expression of *ZmMCM3* (Zy12 vs. EC:  $\log_2FC = 2.7^*$ , AC  
122 vs. Zy24:  $\log_2FC = 1.8^*$ ) and *ZmMCM6* (Zy12 vs. EC:  $\log_2FC = 2.0^*$ , AC vs. Zy24:  
123  $\log_2FC = 2.7^*$ ), marking the onset of DNA replication during S-phase (Maiorano et al.,  
124 2006), peaked in the zygote at 12 HAP, as well as after the first asymmetric zygote  
125 division in the apical cell, which divides more rapidly than the basal cell. The cell  
126 cycle regulatory genes *ZmCycB2;1* (Zy24 vs. Zy12  $\log_2FC = 3.6^*$ ) and *ZmCycB1;2*  
127 (Zy24 vs. Zy12  $\log_2FC = 5.0^*$ ), which mark the G2/M-transition (Maiorano et al.,  
128 2006), were strongly induced at 24 HAP. In contrast to *ZmCycB1;2* (AC/BC vs. Zy12  
129  $\log_2FC > 1.9^*$ ), the expression levels of *ZmCycB2;1* (AC/BC vs. Zy12  $\log_2FC > 5.5^*$ )  
130 were also high in apical and basal cells after zygote division (Sauter et al., 1998). In  
131 summary, these dynamic changes in gene expression (**Figure 1B**) are in perfect  
132 agreement with previous reports, which together with strong correlation between  
133 biological replicates (**Supplemental Figure 2**) assures the high quality and reliability  
134 of our data.

135 Contamination of transcriptomes by RNA from maternal tissues has recently  
136 been discussed as a serious issue that can result in poor reproducibility and  
137 misinterpretation of data sets (Schon and Nodine, 2017). We therefore investigated  
138 the presence of transcripts derived from genes expressed in maternal nucellus tissue  
139 surrounding embryo sacs (Chettoor et al., 2014) to evaluate the possibility of  
140 contamination. None of the nucellus-expressed genes, including GRMZM2G570791  
141 (alpha subunit of DNA-directed RNA polymerase), GRMZM2G125823 (heparanase-  
142 like protein), GRMZM2G099420 (Cinnamoyl CoA reductase), and  
143 GRMZM5G803276 and GRMZM2G336859 (encoding unknown proteins), were  
144 detected in any of our data sets. These results indicate that our data sets are free of  
145 maternal RNA contamination and that the two washing steps were sufficient for  
146 removing maternal RNA from the burst maternal nucellus cells.

147

148 **Comparison of transcriptomic data from maize and rice gametes**

149 A comprehensive comparison of gene expression activity after fertilization has not  
150 been reported yet for any plant species, and the present study thus represents the  
151 first report of global gene expression patterns in gametes, zygotes, and daughter  
152 cells. Therefore, we restricted our comparisons to the transcriptomes of maize and  
153 rice gametes (egg and sperm cells). It was not possible to include the transcriptomes  
154 of *Arabidopsis thaliana* gametes in the comparison, as RNA-Seq data were not  
155 available, and the available microarray data (Borges et al., 2008; Wuest et al., 2010)  
156 could not be accurately normalized to allow us to draw conclusions and lacked  
157 information for thousands of genes. In addition, each gamete in the data set was  
158 measured in a different experiment.

159 We used published RNA-Seq data from rice sperm and egg cells (Anderson et  
160 al., 2013) and initially identified the rice homologs using public databases, i.e.,  
161 EnsemblPlants and RiceAnnotationGenomeProject, which combine data from many  
162 species to identify putative orthologs. If the identity of the homologs/orthologs was  
163 unclear or unknown due to a lack of sequence information, we did not include them  
164 in the comparison. To compare transcription patterns in rice versus maize gametes,  
165 the gene expression values were binned into 200 expression level categories using  
166 the 99<sup>th</sup> percentile per species as the highest category (see also **Supplemental Data**  
167 **Set 4**). We selected the 80 most strongly expressed genes (TOP80 genes) in maize  
168 sperm and egg cells and compared their expression levels with those of the  
169 respective genes in rice (**Figure 2**). A summary of the TOP30 genes of all maize cell  
170 types, including their annotation, is provided in **Supplemental Data Set 5**.

171 Many of the predicted rice homologs/orthologs displayed similar, strong  
172 expression patterns. The proportion of genes with high expression levels was greater  
173 in egg cells than in sperm cells (**Figure 2**). The observation that many predicted rice  
174 homologs/orthologs displayed weaker expression patterns in rice than in maize  
175 might be due to our methods (as we summarized rice ortholog data using the  
176 median), the difficulty in predicting true orthologs within larger gene families, and/or  
177 the lack of common controls to normalize these two studies. Tightly controlled  
178 parallel RNA extraction from cells of different species and the identification of an  
179 appropriate control cell type common to both plant species may improve interspecies  
180 comparisons. However, our comparison pointed to some similarities and general  
181 findings regarding genome activity. Among the TOP80 genes expressed in maize  
182 sperm cells, 10% encode histones and high-mobility group (HMG) proteins (**Figure**

183 **2A**). This finding might explain the strongly condensed, compact sperm cell  
184 chromatin (see also **Figure 1A**). Indeed, a similar observation was reported for rice  
185 sperm cells (Russell et al., 2012b; Anderson et al., 2013). Notably, no chromatin  
186 gene is among the TOP80 genes in maize egg cells. This finding correlates well with  
187 the less condensed chromatin in these cells and the difficulty in staining egg cells  
188 with DAPI (**Figure 1A**). However, in strong contrast to sperm cells, 20% of the  
189 TOP80 genes in maize egg cells encode proteins of the translational machinery,  
190 most of which also displayed similar expression patterns in rice egg cells. These  
191 include two genes encoding the translation initiation factor IF5A (Dresselhaus et al.,  
192 1999a), a gene encoding the translation initiation factor SUI1 (Cui et al., 1998), two  
193 genes encoding the translation elongation factor EF1A (Budkevich et al., 2002), and  
194 many ribosomal protein genes. These observations indicate that sperm cells are  
195 translationally inactive, whereas egg cells are either highly active or well prepared to  
196 strongly enhance translation after being activated during the fertilization process.

197 Another interesting observation relates to transcripts encoding polymorphic  
198 EA1-box proteins and small secreted cysteine-rich proteins (CRPs), which we found  
199 in maize egg cells, but not in sperm cells. The corresponding proteins play key roles  
200 in female gamete cell identity, as well as pollen tube guidance and burst in maize (for  
201 review, see (Dresselhaus et al., 2011; Dresselhaus et al., 2016). However, due to  
202 their polymorphic nature, no unambiguous homologs of the individual members were  
203 identified in the databases from Ensembl Compara or the Rice Genome Annotation  
204 Project. Through manual searches, we identified similar genes in rice (Márton et al.,  
205 2005; Uebler et al., 2015), but true orthologs could not be predicted based on protein  
206 comparisons, and none of the candidate genes have been functionally tested in rice  
207 (**Figure 2B**). However, this finding indicates that genes involved in processes directly  
208 associated with fertilization appear to be polymorphic and specific-specific, thus  
209 representing prime candidate genes involved in speciation mechanisms (Rieseberg  
210 and Willis, 2007).

211

## 212 **Histone variants and chromatin-based gene regulation**

213 Histones are the major protein components of chromatin and, more importantly,  
214 dynamic regulators of transcription. To begin to uncover the molecular basis of  
215 chromatin remodeling and epigenetic reprogramming in plant gametes and the onset  
216 of embryo development, we investigated the expression patterns of histone variants

217 and chromatin assembly factor genes in more detail (**Figure 3, Supplemental Data**  
218 **Set 3G**; important gene families).

219 As mentioned above, some canonical core histones, including two H3 (7 of 17  
220 genes: SP vs. all:  $\log_2FC > 1.5^*$ ) genes and at least three H4 (9 of 15 genes: SP vs.  
221 all:  $\log_2FC > 1.4^*$ ) genes, were predominantly and highly expressed in sperm cells  
222 (**Figure 3B and C**), and may contribute to the compactness of the chromatin and  
223 suggesting that sperm cells are already prepared for S-phase. Moreover, the most  
224 highly expressed gene in sperm, *ZmHmgd1* (SP vs. all:  $\log_2FC > 3.9^*$ ), was  
225 expressed at much higher levels in sperm cells than in any other cell type examined  
226 ( $> \sim 6$ -fold) (**Figure 3F**). *ZmHmgd1* encodes an HMG box protein that plays a role in  
227 chromosome condensation (Thomas and Travers, 2001) and is thought to possess a  
228 role similar to that of histone H1 in chromatin assembly, as both proteins bend linker  
229 DNA at the entry and exit points of the nucleosome. This hypothesis may explain  
230 why linker histone H1 genes are expressed at rather low levels in sperm cells,  
231 although their DNA is densely packed to ensure chromatin stability during sperm  
232 delivery. After fertilization, Hmgd1 appeared to be partially replaced by histone H1,  
233 as the expression of the H1 gene was strongly activated and peaked in 24 HAP  
234 zygotes (9 of 11 genes: Zy24 vs. EC:  $\log_2FC > 1.8^*$ ) (**Figure 3A**), whereas *ZmHmgd1*  
235 (Zy24 vs. SP:  $\log_2FC = -5.0^*$ ) was strongly repressed.

236 The most abundant H3 gene in maize sperm (GRMZM2G145758, SP vs. all:  
237  $\log_2FC > 4.0^*$ ) encodes an unusual replication-independent (RI) H3.3-like variant that  
238 was also predominantly expressed in anthers and was previously designated as  
239 *ZmAPH3*. Phylogenetic analysis showed that *ZmAPH3* is most similar to the  
240 Arabidopsis male gamete-specific histone H3 variant gene *AtMGH3* (Okada et al.,  
241 2005) (**Supplemental Figure 3A**). However, the horizontal distance and the low  
242 number of histone variants and species included in the phylogenetic analysis  
243 suggest that they share a rather distant relationship. All other sperm cell-enriched H3  
244 variants belong to the RI H3.3 group (**Supplemental Figure 3A**) (four orthologous  
245 genes, RI H3.3: SP vs. Zy24:  $\log_2FC > 1.6^*$ ). In Arabidopsis, a limited subset of H3.3  
246 variants referred to as the main HTR (HISTONE THREE-RELATED) protein genes  
247 are predominately expressed in the male gamete (Ingouff et al., 2010). Three  
248 *AtMGH3* homologs and two other RI H3.3 variants are also highly expressed in rice  
249 sperm cells, while other core H3 genes exhibit only limited expression in these cells

250 (Russell et al., 2012a). These findings suggest that RI H3.3 variants encoded by only  
251 a few genes act as major histone H3s in the sperm cells of flowering plants.

252 Two replication-coupled canonical H2As (GRMZM2G151826 and  
253 GRMZM2G041381) exhibited high transcript levels in maize sperm cells, but the  
254 most highly expressed H2A (GRMZM2G149775, SP vs. all,  $\log_2FC > 2.7$ ) belongs to  
255 the RI H2A.Z class (**Supplemental Figure 3B**), which is associated with  
256 nucleosomes at transcription start sites, especially those also containing H3.3 (Deal  
257 and Henikoff, 2011). Therefore, together with histone H3.3 and H2A.Z, which mark  
258 active chromatin via RI nucleosome assembly (Ahmad and Henikoff, 2002; Deal and  
259 Henikoff, 2011), HMGD1 (encoded by *ZmHmgd1*), which likely represents the most  
260 abundant chromatin architectural protein in sperm that binds to highly accessible  
261 regulatory chromatin and active promoters, probably keeps the highly condensed  
262 sperm cell chromatin at least partially accessible. This hypothesis is supported by  
263 our RNA-Seq data set, which includes transcripts of approximately 11,000  
264 differentially upregulated genes in sperm cells versus zygotes at 12 HAP (**Figure**  
265 **4F**), including a subset of TF genes, despite the compact chromatin in sperm cells.

266 Upon fertilization, H3 variants from male and female gametes are actively  
267 removed in Arabidopsis (Ingouff et al., 2010), a scenario that likely also occurs in  
268 maize, as the expression of the canonical core histone repertoire was activated in  
269 conjunction with a dramatic reduction in *H2A.Z*, *H3.3*, and *Hmgd1* expression and a  
270 strong increase in *H1* expression (**Figure 3A**). Thus, it appears that the paternal  
271 chromatin was reprogrammed by newly synthesized and entirely different sets of  
272 histones in the zygote. This theme may even extend to apical and basal cells, since  
273 the list of expressed orthologs of H3 and H4 again shifted to genes different from  
274 those expressed in zygotes.

275 Finally, while the canonical core histones were mostly expressed at very low  
276 levels in egg cells (**Figure 3**), they were induced in zygotes at 12 HAP, indicating the  
277 G1 phase of the cell cycle. Expression peaked in zygotes at 24 HAP, suggesting that  
278 DNA replication was almost complete (**Figure 3**). These observations support the  
279 hypothesis that the egg cell is arrested and requires activation after gamete fusion.  
280 Thus, chromatin-based transcriptional reprogramming in the zygote may represent a  
281 key step in MZT and the initiation of the sporophytic generation.

282

283 **ZGA occurs shortly after fertilization in maize**

284 To identify the global onset of ZGA, it is important to examine the transcriptomes of  
285 both gametes, i.e., egg and sperm cells, as well as zygotes at different stages. We  
286 therefore investigated zygotes collected at 12 and 24 HAP. At 12 HAP, i.e., only ~4 h  
287 after fertilization, all egg cells were fertilized, as indicated by the presence of  
288 degenerated receptive synergid cells. These egg cells were considered to represent  
289 early zygotes. We chose to investigate zygotes at 24 HAP, as they appeared to be  
290 activated at this point, as indicated by the duplication of DNA content (**Figure 1A**). At  
291 later time points after pollination, the zygotes underwent mitosis, but the stages  
292 appeared less synchronous than those at earlier time points. We chose genes with  
293 an  $\text{abs}(\log_2\text{FoldChange}) > 1$  and adjusted  $p\text{-value} < 0.05$  in the respective comparison  
294 as genes with a potential biological function and determined whether they were  
295 induced or repressed. Based on these criteria, sperm cells formed the most distinct  
296 group, expressing 4,090 differentially upregulated genes in all comparisons (**Figure**  
297 **4F**). As all of the other cell types are similar, fewer genes were induced in these cells  
298 compared to all other cell types; 482 differentially upregulated genes were detected  
299 in egg cells in all comparisons, 109 were detected in zygotes at 12 HAP, 31 were  
300 detected in zygotes at 24 HAP, and 6 and 8 were detected in apical and basal cells,  
301 respectively (**Figure 4F, Supplemental Data Set 6**).

302 We compared zygotes at 12 HAP to both sperm and egg cells and identified  
303 3,605 induced genes (9.1% of the maize transcriptome of 39,469 annotated genes;  
304 Schnable et al., 2009) over all chromosomes shortly after fertilization (**Figure 4B**).  
305 This high number of activated genes indicates that global ZGA in maize already  
306 occurs in the early zygote and not several days after fertilization, as previously  
307 reported (Grimanelli et al., 2005). Although *de novo* transcription has also been  
308 observed in Arabidopsis zygotes (e.g., Autran et al., 2011; Nodine and Bartel, 2012;  
309 Del Toro-De León et al., 2014), the timing of global ZGA in this species is unclear,  
310 and some reported results are currently under debate due to contamination from  
311 maternal tissues (Schon and Nodine, 2017).

312 We compared zygotes at 12 HAP with sperm and egg cells and identified  
313 7,356 and 1,933 induced genes, respectively (**Figure 4B**). Furthermore, we identified  
314 1,730 differentially upregulated genes in sperm and egg cells versus zygotes at 12  
315 HAP (**Figure 4A**), which can also be viewed as genes downregulated in zygotes at  
316 12 HAP compared to gametes. These findings also suggest that major  
317 rearrangements in the transcriptome occur following fertilization.

318 To obtain a global overview of transcriptome dynamics during zygote  
319 development, we defined various gene expression profiles as capturing not only on  
320 and off states, but also the induction or repression of genes during the transition from  
321 gametes to zygotes and their descendant cells (**Figure 4E, Supplemental Data Set**  
322 **6**). Very specific gene expression profiles were found for egg cells: 326 genes were  
323 upregulated in this cell type, whereas 95 genes were downregulated. Shortly after  
324 fertilization, 356 and 1,510 genes were transiently induced only in zygotes at 12 HAP  
325 and in zygotes at both stages, respectively. Approximately 10% of the genes in each  
326 group encode transcriptional regulators. Of the 3,808 genes induced after  
327 fertilization, 223 were predominantly expressed in apical cells, whereas 182 were  
328 predominantly expressed in basal cells. These results indicate that the expression  
329 levels of many genes are higher in the zygote than in its progenitor cells, supporting  
330 the notion of an early onset for ZGA. Few genes were transiently repressed after  
331 fertilization (137 genes). Together, these findings reveal a highly dynamic  
332 transcriptional landscape after fertilization in maize and demonstrate that ZGA  
333 occurs shortly after fertilization in this plant. Studies involving pollination with other  
334 inbred lines are now needed to distinguish between maternal and paternal  
335 transcripts and thus to determine whether both genomes contribute equally to ZGA  
336 in this species.

337

### 338 **Transcription factor activation schemes in gametes and zygotes**

339 As TFs are major regulators of gene expression, we next examined TF gene  
340 expression levels in gametes and early zygotic embryos based on the maize TF  
341 database Grassius ([www.grassius.org](http://www.grassius.org)). Across all cell types, 1,478 of 2,630 maize  
342 TF genes were expressed in gametes and zygotes ( $\log_2FC > 1$  and  $p_{adj} < 0.05$  in at  
343 least one comparison). Comparing their transcription levels during early development  
344 (**Figure 5A, Supplemental Data Set 3**) showed that zygotes formed a group distinct  
345 from apical and basal cells, and that both groups differed from gametes. We  
346 identified 428 TF genes that were induced in zygotes (12 and 24 HAP), 189 of which  
347 were strongly activated shortly after fertilization (Zy12 vs. SP and EC,  $\log_2FC > 3$ ). We  
348 detected 25 TF genes specifically expressed in pro-embryonic cells. Only 23  
349 paternal and 103 maternal TF genes were expressed at similar levels in gametes  
350 and zygotes (**Supplemental Data Set 3**). While we could not distinguish between  
351 paternal and maternal mRNAs in our assays and were thus unable to identify the

352 maternal-to-zygotic transition (MZT) (Baroux and Grossniklaus, 2015), the results  
353 suggest that approximately 8.6% (25+103/1,478) of expressed TF genes are  
354 parentally transmitted, while 29% (428/1,478) are newly or more intensely  
355 transcribed in maize zygotes. These data support the notion that TF genes are  
356 activated early in maize zygotes (at 12 HAP; 403 of 428 TF genes were induced in  
357 zygotes vs. 25 of 428 at 24 HAP) (**Figure 5A**).

358 We then identified important TF classes from the various expression profiles  
359 (**Supplemental Data Set 6**; profiles of TF classes are summarized in **Supplemental**  
360 **Data Set 7**). In sperm cells, many genes belong to the TF class AT-rich interactive  
361 domain (ARID 5/10) proteins. Members of this class have been implicated in sperm  
362 cell development in plants and mammals. In Arabidopsis, ARID1 is necessary for the  
363 appropriate expression of DUO1, a major TF required for sperm cell formation  
364 (Zheng et al., 2014). In mice, the loss of ARID4A combined with ARID4B  
365 haploinsufficiency leads to spermatogenic arrest (Wu et al., 2013). In egg cells, we  
366 detected high proportions of TFs from the classes FAR1-like (3/15), mTERF (8/30),  
367 Sigma70-like (2/9), S1Fa-like (2/2), and GeBP (5/21) compared to the other cell  
368 types analyzed. The first four classes are related to plastid development (Zhou et al.,  
369 1995; Ouyang et al., 2011; Kleine, 2012; Wei et al., 2012). This finding suggests that  
370 a tightly controlled regulatory network controls plastid development during the first  
371 steps in the plant life cycle. Members of the GL1 enhancer binding protein (GeBP)  
372 class of leucine-zipper TFs have been linked to the cytokinin response in  
373 Arabidopsis and are thought to be mainly expressed in vegetative meristems and in  
374 the primordia of young leaves (Chevalier et al., 2008). Our data suggest that this  
375 class of TFs also plays a role in the transition from egg cells to early zygotes.

376 As discussed above, at the first zygotic time point (12 HAP), genes for many  
377 TF classes were induced (**Supplemental Data Set 7**). The auxin-responsive ARF  
378 TFs (7/38) and the ethylene-responsive AP2-EREBP TFs (34/212) might be  
379 important at this stage, as crosstalk between these pathways is thought to be  
380 essential during zygote and pro-embryo development (see below). In addition, many  
381 genes from the TF classes C3H/CCCH (18/54), Trihelix (11/41), ZIM (10/36), MADS  
382 (15/77), NAC (26/134), bZIP (24/128), and Homeobox (26/133) were induced at this  
383 time point. MADS-box TFs are associated with reproductive organ development and  
384 play a role in gametes and in zygotic embryogenesis (Schreiber et al., 2004; Lehti-  
385 Shiu et al., 2005).

386

### 387 **Activation of embryo patterning**

388 After ACD, *WOX* genes encoding homeodomain TFs mark apical and basal cell fate  
389 upon zygote division in Arabidopsis (Breuninger et al., 2008). In maize, *ZmWOX9A*  
390 and *ZmWOX9B* likely represent the homologs of *AtWOX8* and *AtWOX9*, respectively  
391 (Salvo et al., 2014). Both *ZmWOX9A* and *ZmWOX9B* were induced shortly after  
392 fertilization (Zy12 vs. SP/EC:  $\log_2FC > 5.9^*$  and  $7.0^*$ , respectively) and were  
393 expressed at higher levels in basal cells than in apical cell, like their counterparts in  
394 Arabidopsis (**Figure 5B, Supplemental Data Set 3B**), indicating that they might play  
395 a similar role in early embryonic patterning. However, unlike *AtWOX2*, which marks  
396 apical descendants of the zygote, *ZmWOX2A* was expressed at very low levels in  
397 basal cells, with almost no expression in apical cells. Instead, this gene was  
398 expressed much later during seed development in the endosperm (Maize eFP  
399 Browser at bar.utoronto.ca). This finding indicates that pattern formation regulated by  
400 *ZmWOX2A* and other genes likely occurs later in maize embryogenesis than in  
401 Arabidopsis embryogenesis (Zhao et al., 2017). Notably, *ZmWOX13A* is the only  
402 *WOX* gene that was transcribed at high levels in sperm cells (SP vs. all:  
403  $\log_2FC > 4.3^*$ ); whether it marks cell identity of the male gamete or represents a  
404 zygote activator remains to be investigated. In Arabidopsis, *BBM* and *LEC* TF genes  
405 are key players in embryogenesis, and the presence of either gene is sufficient to  
406 induce competence for embryogenesis (Lotan et al., 1998; Boutilier et al., 2002).  
407 Overexpressing a combination of the maize homologs *WUS2* and *BBM* was recently  
408 shown to significantly increase embryogenic potential in tissue culture and thus  
409 represents a key mechanism to increase the transformation efficiency in maize  
410 (Lowe et al., 2016). Notably, the maize homologs *ZmBBML1* (Zy12 vs. SP/EC:  
411  $\log_2FC > 10.5^*$ ), *ZmBBML2* (Zy12 vs. SP/EC:  $\log_2FC > 10.2^*$ ), and *ZmLEC1* (Zy12 vs.  
412 SP/EC:  $\log_2FC > 7.9^*$ ) were already induced at 12 HAP (**Figure 5B**), suggesting that  
413 the egg cell quickly acquires embryogenic competence and that the characteristic  
414 embryogenic transcription program is activated shortly after fertilization. *ZmBBML3*  
415 was induced in zygotes at 24 HAP (Zy24 vs. Zy12:  $\log_2FC = 6.5^*$ ) and after zygote  
416 division (AP/BC vs. Zy24:  $\log_2FC = 3.5/3.9^*$ ), suggesting step-by-step activation of the  
417 embryonic program. A comparison of apical and basal cells with zygotes at 24 HAP  
418 revealed 2,228 genes induced in both cell types, 832 induced only in apical cells,  
419 and 485 induced only in basal cells (**Figure 4D**). This induction was accompanied by

420 the downregulation of 2,182 genes in apical and basal cells versus zygotes at 24  
421 HAP (**Figure 4C**). These data suggest that global rearrangements also occur in the  
422 transcriptomes of apical and basal cells compared to their predecessor.

423 The development of multicellular organisms often involves ACDs to generate  
424 daughter cells with different cell fates. Spindle positioning is particularly associated  
425 with the generation of symmetric or asymmetric cell fates (Siller and Doe, 2009). The  
426 MATH-BTB domain protein ZmMAB1, a component of a CUL3-E3 ubiquitin ligase  
427 complex, regulates spindle length during the development of the male and female  
428 germline in maize (Juranic et al., 2012). ZmMAB1 may also function like its animal  
429 homolog, the key ACD regulator MEL-26, a factor required for embryogenic  
430 morphogenesis that regulates the formation of mitotic spindles in the early embryo  
431 (Pintard et al., 2003). As shown in **Figure 5C**, MAB family genes were strongly  
432 upregulated (*ZmMAB1-3*, *ZmMAB6* and *ZmMAB24*, *Zy12* vs. SP:  $\log_2FC >1.5$  to  
433  $10.7^*$ ) after fertilization in maize. The highest expression levels of these genes were  
434 detected in zygotes at 24 HAP (**Supplemental Data Set 3A**; important gene  
435 families), suggesting that they play roles in processes such as spindle positioning  
436 during the first asymmetric zygote division (*ZmMAB2-3*, *Zy24* vs. *Zy12*  $\log_2FC=3.1^*$   
437 and  $1.8^*$  respectively). Functional studies of *ZmMABs* are now needed to investigate  
438 this hypothesis.

439

#### 440 **Cell cycle regulation during zygote development**

441 Since previous reports provide only a glimpse of cell cycle regulation in plant  
442 gametes and during zygote development, we investigated the expression patterns of  
443 important cell cycle regulator genes. First, we searched for orthologs of Arabidopsis  
444 cell cycle genes (Vandepoele et al., 2002) and then included cyclins and other cell  
445 cycle-related factors described previously for maize (see Methods), resulting in a list  
446 of 89 cell cycle genes (**Supplemental Data Set 3**). As shown in **Figure 6A**,  
447 hierarchical clustering of these genes from different cell types clearly separated  
448 sperm cell genes from a group of genes from egg cells and zygotes at 12 HAP. The  
449 expression patterns of the genes from zygotes at 24 HAP were more similar to those  
450 of apical and basal cells.

451 The G1-phase of sperm cells is characterized by high expression levels of  
452 *Cdc27*-like genes (GRMZM2G148626, GRMZM2G005536, SP vs. all:  $\log_2FC>5.7^*$ )  
453 encoding subunits of the APC complex, which controls CDK degradation in M- and

454 G1-phase, and relatively low levels of CDK gene expression. Furthermore,  
455 retinoblastoma-related protein genes *RBR1* and *RBR2* were highly expressed in  
456 sperm cells (**Figure 6A**, SP vs. all:  $\log_2FC > 2.9^*$ ). *RBR1* and *RBR2* mediate G1-  
457 phase arrest by inhibiting E2F TFs, which in turn promote DNA replication (Sabelli et  
458 al., 2013). Compared to the other cell types, egg cells showed by far the lowest  
459 expression levels of cell cycle genes and lacked a typical cell cycle phase-specific  
460 gene expression pattern. This finding, together with the results of cell cycle gene  
461 expression analysis and the microscopy evidence reported above (**Figure 1**),  
462 indicate that the egg cell is in a resting G0 stage rather than in G1 (**Figure 6B**).  
463 Thus, the egg cell must be activated and its cell cycle synchronized with the sperm  
464 cell cycle stage before karyogamy (fusion of both nuclei) is executed. A typical G1-  
465 phase expression pattern was observed in zygotes at 12 HAP (**Figure 6A**), with  
466 slightly upregulated expression of E2F TF genes (GRMZM2G060000,  
467 GRMZM2G361659, GRMZM2G378665, Zy12 vs. EC,  $\log_2FC > 2.5^*$ ) and (especially)  
468 their cell cycle target genes (**Supplemental Data Set 3**). The latter include mini-  
469 chromosome maintenance genes (*ZmMCM3-6*, Zy12 vs. EC:  $\log_2FC > 2.0^*$ ),  
470 encoding DNA-replication licensing factors required for replication initiation, and the  
471 gene encoding proliferating cell nuclear antigen (PCNA), which acts as a scaffold to  
472 recruit proteins involved in DNA replication and repair (Sabelli et al., 2009; Tuteja et  
473 al., 2011). Notably, *RBR3*, encoding an activating factor of *MCM2-7* transcription,  
474 was specifically induced in zygotes at 12 HAP (Zy12 vs. EC:  $\log_2FC = 2.2^*$ ), while  
475 *RBR1* and *RBR2*, two genes encoding repressors of E2F TFs, were repressed in  
476 these zygotes compared to sperm cells (Zy12 vs. SP:  $\log_2FC < -3.8^*$ ). This  
477 expression pattern coincided with the induction of CDK A genes (Zy12 vs. SP:  
478  $\log_2FC > 1.1$  to  $7.0^*$ ) and low levels of expression of CDK B genes, indicating that  
479 fertilized egg cells had been activated and zygotes at 12 HAP were in G1-phase.  
480 *MCM2-7* expression levels were lower in zygotes at 24 HAP versus 12 HAP,  
481 whereas CDK B2 genes (9 of 14 genes, Zy24 vs. Zy12:  $\log_2FC > 2.8^*$ ) and B-type  
482 cyclin genes were induced (8 of 9 genes, Zy24 vs. Zy12:  $\log_2FC > 1.9^*$ ), especially  
483 *ZmCycB1;2*, suggesting that S-phase was completed and the zygotes were prepared  
484 for the G2/M-phase transition (Meijer and Murray, 2001). M-phase took place at 27–  
485 35 HAP (**Figure 1A**). Notably, G1-phase markers such as *MCM2-7* were expressed  
486 at slightly higher levels in apical versus basal cells, hinting at more rapid cell cycle  
487 progression in the apical cell after ACD.

488 Taken together, our cell cycle analysis by microscopy of DNA staining  
489 patterns, transcription data from selected gene sets, and global cell expression  
490 analysis of cell cycle genes allowed us to determine the timing of zygote  
491 development in maize (**Figure 6B**). On average, fertilization occurs at ~8 HAP.  
492 Sperm cells appear in G1-phase, and egg cells are in a resting G0-phase of the cell  
493 cycle. Activated zygotes are in G1 phase at 12 HAP (~4 h after fertilization) and at  
494 G1/S-phase at 24 HAP. Mitosis typically occurs at 26–36 HAP, and cytokinesis lasts  
495 until 44 HAP. ACD is completed between 44 and 50 HAP, generating both apical and  
496 basal cells in G1-phase.

497

### 498 **The role of auxin in early embryogenesis in maize**

499 To demonstrate the utility of our data sets, we chose the auxin pathway, which plays  
500 a key role in early embryo patterning in Arabidopsis, as an example for analysis.  
501 Auxin gradients generated by PIN efflux carrier proteins establish the apical-basal  
502 axis upon the first ACD in the Arabidopsis zygote (Friml et al., 2003). The molecular  
503 mechanisms that determine axis formation during early embryogenesis in monocots  
504 are largely unknown. We therefore analyzed the expression of auxin biosynthesis,  
505 transport, and response genes, as shown in **Figure 7 (Supplemental Data Set 3D;**  
506 **important gene families)**. In maize, the earliest ZmPIN1a localization was observed  
507 at 6 DAP at the adaxial side of the embryo proper (Chen et al., 2014). To identify  
508 potential PIN proteins that function at the earliest stage of embryo patterning, we  
509 analyzed the expression of all *PIN* family genes. Among the 15 *PIN* genes in maize  
510 (Yue et al., 2015), only *ZmPIN8* was weakly expressed in the zygote and  
511 upregulated after ACD in both apical and basal cells (AC/BC vs. Zy12:  
512  $\log_2FC=3.8/3.7^*$ ). A number of *ZmABCBs*, representing potential auxin transporter  
513 genes (Yue et al., 2015), were also active in maize gametes and/or zygotes. Auxin  
514 biosynthesis genes *ZmTAR1* (Zy12 vs. SP/EC:  $\log_2FC>1.2^*$ ) and *ZmYUC3* (Zy12 vs.  
515 EC:  $\log_2FC=9.4^*$ ) were significantly induced after fertilization, with higher expression  
516 levels in basal cells versus apical cells (*ZmTAR1* BC vs. AC:  $\log_2FC=1.4^*$ ). Auxin  
517 receptor genes *ZmABP1*, *ZmABP4*, and *ZmABPL* were also expressed in egg cells  
518 (EC vs. SP:  $\log_2FC>1.1^*$ ) but not in sperm cells and became transiently activated  
519 after fertilization (Zy12 vs. SP:  $\log_2FC>1.9^*$ , AC/BC vs. Zy24:  $\log_2FC< -1.4^*$ ). Of the  
520 auxin responsive factor (*ARF*) genes examined, *ZmARF7* had the highest  
521 expression level in the egg cell and was almost completely switched off after

522 fertilization (EC vs. SP/Zy12/Zy24:  $\log_2FC > 3.1^*$ , AC/BC vs. EC:  $\log_2FC < -4.1^*$ ).  
523 Other *ARF* genes, such as *ZmARF8*, 13, 17, and 28, were expressed at similar  
524 levels in all cells except sperm cells. In general, *ARF* transcript levels were higher in  
525 the apical daughter cell of the zygote than in the other daughter cell (**Figure 7B**:  
526 AC/BC vs. Zy24). A few *AUX/IAA* repressor genes encoding proteins that interact  
527 with *ARF* regulators were activated after fertilization (**Figure 7B**: Zy12 vs. SP/EC). In  
528 particular, *ZmIAA17* (Zy12 vs. SP/EC  $\log_2FC > 4.3$ ) was transiently expressed only  
529 shortly after fertilization; *ZmIAA17* might be involved in the inactivation of *ZmARF17*-  
530 regulated gene expression patterns. Another highly upregulated gene, *ZmSAUR7*  
531 (Zy12 vs. SP/EC:  $\log_2FC > 5.2^*$ , AC/BC vs. Zy12:  $\log_2FC < -2.6^*$ ), is one of 79 SAUR  
532 (*SMALL AUXIN UP RNAs*) genes in maize, representing the largest family of auxin  
533 response genes (Ren and Gray, 2015). Globally, we found that auxin pathway genes  
534 were highly induced in the early zygote at 12 HAP and expressed at decreasing  
535 levels from 24 HAP zygotes to apical and basal cells (**Figure 7B**). By contrast, in  
536 Arabidopsis, these genes continue to show a strong auxin response, especially in  
537 the apical cell after ACD (for review, see Petrášek and Friml, 2009). Moreover,  
538 transcripts encoding homologs of key players in auxin-regulated early embryo  
539 patterning in Arabidopsis, such as *ARF5* (MP), *IAA12* (BDL), *PIN1*, and *PIN7*, were  
540 absent in zygotes and their daughter cells in maize.

541 The observation that gametes and early zygotes are equipped with transcripts  
542 encoding proteins for auxin biosynthesis, transport, and perception, as well as the  
543 identification of strongly regulated auxin response genes (**Supplemental Data Set**  
544 **8**), indicates that auxin-regulated early embryo patterning is likely different in maize  
545 and other grasses compared to Arabidopsis, providing an entry point for investigating  
546 the role of this important hormone during early embryogenesis in grasses. In addition  
547 to auxin signaling, we also obtained hints about brassinosteroid and ethylene  
548 signaling during early embryo development in maize, which will be investigated in the  
549 future.

550

### 551 **Cell signaling during fertilization and early embryogenesis**

552  $Ca^{2+}$  signaling is thought to play a pivotal role in fertilization by regulating a plethora  
553 of cellular processes (Chen et al., 2015). Annexins are a class of  $Ca^{2+}$ -regulated  
554 proteins that link  $Ca^{2+}$  signaling to membrane and cytoskeleton dynamics (Gerke et  
555 al., 2005). Of the 12 genes encoding annexins in maize (Zhang et al., 2015),

556 *ZmAnn6* and *ZmAnn7* exhibited very high, transient expression in egg cells (EC vs.  
557 SP:  $\log_2FC=8.5/2.1^*$ , EC vs. Zy12:  $\log_2FC=1.1/-^*$ ) and early zygotes (AC/BC vs.  
558 Zy12:  $\log_2FC< -4.1/-3.2^*$ ), respectively (**Figure 8A, Supplemental Data Set 3C**;  
559 important gene families). Thus, these proteins might function as key players in intra-  
560 and intercellular  $Ca^{2+}$  signaling during fertilization and early embryo development.

561 Signal perception and transduction through cell-surface receptor-like kinases  
562 (RLKs) likely play also roles in gamete interaction, fertilization, and early seed  
563 development in plants. We detected at least three RLK genes that were preferentially  
564 expressed in sperm cells (GRMZM2G011806, GRMZM2G016480,  
565 GRMZM2G428554, SP vs. EC/Zy12/Zy24:  $\log_2FC>2.3^*$ ) (**Figure 8B, Supplemental**  
566 **Data Set 3E**; important gene families), representing potential players in gamete  
567 recognition and/or sperm activation. We did not identify RLK genes that were  
568 preferentially expressed in egg cells. In Arabidopsis, *SOMATIC EMBRYOGENESIS*  
569 *RECEPTOR KINASE1* (*AtSERK1*) is expressed in developing ovules and early  
570 embryos, and enhances embryonic competence in cell culture (Hecht et al., 2001).  
571 While its maize ortholog *ZmSERK1* (Salvo et al., 2014) was expressed at very low  
572 levels in gametes and zygotes, *ZmSERK2* and *ZmSERK3* were expressed in  
573 zygotes (e.g., *ZmSERK3* Zy12 vs. EC:  $\log_2FC=3.7^*$ ) and daughter cells (**Figure 8C**),  
574 indicating the involvement of similar signaling pathways in embryonic initiation.  
575 Moreover, several *RLK* genes (GRMZM2G038165, GRMZM2G428554,  
576 GRMZM2G089461) were upregulated and differentially expressed in apical and  
577 basal cells (AC/BC vs. Zy24:  $\log_2FC>1.5^*$ ), thus representing exciting candidates for  
578 future functional studies investigating cellular communication during early embryo  
579 development in grasses.

580

## 581 **Conclusions**

582 Detailed analysis of global gene expression patterns in plant gametes, zygotes, and  
583 manually separated apical and basal cells has allowed the onset of global ZGA in  
584 maize to be determined for the first time. The observation that ZGA occurs soon after  
585 fertilization, displaying a highly dynamic and partially transient pattern, is surprising  
586 and contradicts previous studies using a limited number of genes. These studies  
587 indicated that the zygote is in a relatively quiescent transcriptional state, that only a  
588 few genes are *de novo* activated in the zygote, and that ZGA occurs gradually rather  
589 than all at once (Baroux and Grossniklaus, 2015; Zhao and Sun, 2015). The striking

590 differences in the expression patterns of cell cycle regulators between sperm and  
591 egg cells coincide with a distinct chromatin state in sperm cells and define a  
592 quiescent cell cycle state in egg cells, although egg cells appear to be translationally  
593 highly active or well prepared to quickly activate the translational machinery after  
594 fertilization. The chromatin state in sperm appears to depend on replication-  
595 independent histone assembly and the HMG protein ZmHmgd1, which likely keeps  
596 the highly condensed sperm cell chromatin at least partially accessible, as  
597 demonstrated by the numerous transcribed genes. In addition, our data allowed us to  
598 differentiate between the stages during G1-phase that occur in zygotes at 12 HAP,  
599 apical cells, and basal cells, and they suggest a preference for certain CDKs and  
600 cyclins during the first two cell cycles in plants. Analysis of the expression levels of  
601 TFs, structural regulators, and signaling pathway genes allowed us to identify  
602 relevant genes homologous to key, well-known Arabidopsis regulators as well as  
603 novel candidate genes, which will serve as a starting point for many future studies.

604 In summary, our analyses of the genes described above represent only a few  
605 examples of how our comprehensive dataset can be used. This gene expression  
606 atlas should further accelerate the identification of key players involved in many  
607 biological processes, including fertilization, early embryogenesis, and the cell cycle,  
608 as well as the translational machinery. In addition, our data set could be used to  
609 uncover genes (and their corresponding promoters) for use in future efforts aimed at  
610 increasing seed yield and quality in maize and other crops.

611

612

## 613 **METHODS**

### 614 **Plant materials and growth conditions**

615 Maize (*Zea mays*) inbred line B73 was cultivated in a walk-in plant growth room at  
616 26°C under illumination of 24,000 lux using alternating SON-T Agro and HPI-T Plus  
617 bulbs with a 16 h light/8 h dark cycle and a relative humidity of 60%. Flowers at  
618 anthesis and pollinated cobs were used to isolate cells for RNA-Seq.

619

### 620 **Isolation of cells from male and female gametophytes**

621 Hundreds of maize plants were grown to collect sufficient numbers of manually  
622 isolated cells. Each biological replicate consisted of pooled cells from different

623 plants. Only the middle part of the cob was used for cell isolation from excised  
624 ovules. A whole cob was used to isolate cells at a defined developmental stage.  
625 Sperm cells were released from maize pollen grains (male gametophytes) by  
626 osmotic shock and separated using density gradient centrifugation on a  
627 discontinuous Percoll gradient. The detailed protocol is given below. Egg cells were  
628 isolated from embryo sacs (female gametophytes) of unpollinated ovules as  
629 described (Kranz et al., 1991). Early and late developmental stage zygotes were  
630 isolated from ovules at 12 hours after pollination (HAP) and 24 HAP, respectively, as  
631 previously described (Cordts et al., 2001). Apical and basal cells were dissected  
632 from two-celled proembryos isolated from ovules at between 48-52 HAP following  
633 the procedure used for zygotes with some modifications (described in detail below).  
634 All cells isolated from ovules were individually collected using a microcapillary and  
635 washed twice in mannitol solution (480 mOsmol·kg<sup>-1</sup> H<sub>2</sub>O). Cells showing  
636 cytoplasmic streaming were individually transferred to 0.5 ml Eppendorf RNA/DNA  
637 LoBind microcentrifuge tubes, immediately frozen in liquid nitrogen, and stored at  
638 -80°C for mRNA extraction. Three biological replicates (each representing an  
639 independent pool of cells) were carried out, each with ~1,000 sperm cells, 20 egg  
640 cells, 14 to 15 zygotes at 12 HAP, 16 to 17 zygotes at 24 HAP, 16 apical cells, and  
641 13 to 14 basal cells (**Table 1**). All three biological replicates of each cell type were  
642 used for RNA-Seq and subsequent transcriptome analyses.

643

#### 644 **Sperm cell isolation**

645 Sperm cells were isolated as described (Dupuis et al., 1987) with some  
646 modifications. Pollen grains were collected upon shedding, immersed in 550  
647 mOsmol·kg<sup>-1</sup> H<sub>2</sub>O mannitol solution (100 mg pollen/ml solution), and incubated on a  
648 platform shaker with slow agitation (80 rpm) for 1 h. The resulting lysate was filtered  
649 through a 40 µm cell strainer to remove exines and unruptured pollen grains,  
650 resulting in a yellowish filtrate containing sperm cells and starch granules. A Percoll  
651 gradient was prepared in a 30 ml COREX tube, consisting of 5 ml 30% (v/v) Percoll  
652 in 550 mOsmol·kg<sup>-1</sup> H<sub>2</sub>O mannitol solution at the bottom, 6 ml 20% (v/v) Percoll in  
653 550 mOsmol·kg<sup>-1</sup> H<sub>2</sub>O mannitol solution in the middle, and 6 ml 15% (v/v) Percoll in  
654 550 mOsmol·kg<sup>-1</sup> H<sub>2</sub>O mannitol solution at the top. Sperm-containing filtrate (10 ml)  
655 was layered on top of the Percoll gradient and centrifuged in a swing-out rotor at

656 12,000xg for 1 h at 4°C. After centrifugation, distinct white layers were visible in the  
657 15/20% Percoll interphase and the 20/30% Percoll interphase. The 20/30%  
658 interphase, which was enriched in sperm cells, was carefully aspirated using a  
659 Pasteur pipette and transferred to 15 ml or 50 ml Falcon tubes. At least 10 volumes  
660 of fresh 550 mOsmol·kg<sup>-1</sup> H<sub>2</sub>O mannitol solution were added to the sperm cell-  
661 enriched fraction, and the cells were washed by carefully inverting the tube several  
662 times. The sperm cells were pelleted by centrifugation at 2,500xg for 15 minutes at  
663 4°C and the supernatant was removed without disturbing the pellet, leaving a volume  
664 of approximately 50–100 µl. The pellet was resuspended in the remaining  
665 supernatant by careful pipetting, resulting in a solution highly enriched in sperm cells.  
666 Cell counting was performed using a Neubauer counting chamber. Isolated sperm  
667 cells were used immediately or shock-frozen in liquid nitrogen and stored at -80°C.

668

#### 669 **Isolation of apical and basal cells**

670 To identify the time point of asymmetric cell division (ACD) of the zygote, several  
671 cobs were pollinated and analyzed at different intervals after pollination. The first  
672 zygotes were analyzed at 24 HAP. Subsequent examinations were performed at 1-h  
673 intervals; on average, zygote ACD was observed at ~48 HAP. Apical and basal cells  
674 were subsequently separated using cell wall degrading enzyme solution containing  
675 1.5% Driselase (Sigma), 1.5% pectinase (Fluka), 0.5% pectolyase Y23 (Karlan),  
676 1.0% hemicellulase (Sigma), 1.0% cellulase “Onozuka R10” (Serva), and 1.5%  
677 maceroenzyme (Karlan) in mannitol solution (480 mOsmol·kg<sup>-1</sup> H<sub>2</sub>O). The enzyme  
678 solution (100 µl) was combined with 1 ml mannitol solution (480 mOsmol·kg<sup>-1</sup> H<sub>2</sub>O),  
679 and ovary sections containing embryo sacs at 48 HAP were incubated in the diluted  
680 enzyme solution for 30 min at room temperature, followed by manual dissection of  
681 two-celled proembryos. The attachment between the apical and basal cell  
682 protoplasts was gently touched with a very thin glass needle to separate both cells.  
683 The cells were washed twice in mannitol solution (480 mOsmol·kg<sup>-1</sup> H<sub>2</sub>O), collected  
684 in 0.5 mL Eppendorf RNA/DNA LoBind microcentrifuge tubes, immediately frozen in  
685 liquid nitrogen, and stored at -80°C for mRNA isolation.

686

#### 687 **RNA extraction, cDNA preparation and purification**

688 The mRNA was extracted from cell samples using a Dynabeads mRNA DIRECT  
689 Micro Kit (Life Technologies). A SMARTer Ultra Low RNA Kit for Illumina  
690 Sequencing (Clontech Laboratories) was used to generate first-strand cDNA.  
691 Double-stranded cDNA was amplified by LD PCR (15 cycles) and purified via  
692 magnetic bead cleanup using an Agencourt AMPure PCR Purification Kit (Beckman  
693 Coulter). The quality of the purified cDNA was measured using an Agilent 2100  
694 Bioanalyzer with an Agilent High Sensitivity DNA Kit (Agilent Technologies), frozen in  
695 liquid nitrogen, and stored at  $-80^{\circ}\text{C}$ .

696

### 697 **Library construction and Illumina sequencing**

698 Library preparation was carried out as described in the Adapted Nextera Sample  
699 Preparation protocol (Clontech Laboratories) for use with the SMARTer Ultra Low  
700 RNA Kit for Illumina Sequencing. Input cDNA (5 ng) was tagmented (tagged and  
701 fragmented) via the Nextera transposome. The products were purified and amplified  
702 via a limited-cycle PCR program to generate multiplexed sequencing libraries. The  
703 libraries were quantified using a KAPA SYBR FAST ABI Prism Library Quantification  
704 Kit (Kapa Biosystems). Equimolar amounts of each library were pooled and used for  
705 cluster generation on the cBot system with Illumina TruSeq PE Cluster v3 and  
706 Illumina TruSeq Dual Index Sequencing Primer paired end kits. Sequencing runs  
707 were performed on a HiSeq 1000 instrument using the dual indexed 2 x 100 cycles  
708 paired end (PE) protocol and TruSeq SBS v3 reagents according to the Illumina  
709 HiSeq 1000 System User Guide. Image analysis and base calling resulted in .bcl  
710 files, which were converted into .fastq files with CASAVA1.8.2 software. Library  
711 preparation and Illumina sequencing runs were performed at the Genomics Core  
712 Facility “KFB - Center for Fluorescent Bioanalytics” ([www.kfb-regensburg.de](http://www.kfb-regensburg.de)). The  
713 raw data (.fastq) plus supplemental tables, including count and TPM data for all  
714 replicates was uploaded to GEO and is available under accession number  
715 GSE98379.

716

### 717 **Bioinformatic and statistical analyses**

718 *(I) Quality control and alignment.* The quality of sequencing data from the RNA-Seq  
719 libraries was assessed with FASTQC  
720 (<http://www.bioinformatics.babraham.ac.uk/projects/fastqc/>). Primer contamination  
721 from the SMARTer Ultra Low RNA Kit was removed with cutadapt (ver.1.13; Martin,

722 2011). Size and quality trimming were then performed using Trimmomatic (ver. 0.32  
723 (Am et al., 2014), ILLUMINACLIP: NexteraPE-PE\_SMARTer.fa:2:30:10:2:true  
724 TRAILING:26 LEADING:26 MINLEN:25). The results from trimming are summarized  
725 in **Supplemental Table 1** (mapping information). Trimmed reads were aligned to the  
726 maize genome (AGPv3, INSEC Assembly GCA\_000005005.5, release 23,  
727 ftp://ftp.ensemblgenomes.org/pub/plants/). STAR (Dobin et al., 2013) was used to  
728 align the mRNA reads. Alignment statistics are summarized in **Supplemental Table**  
729 **1**. Duplicate reads were identified with picard MarkDuplicates  
730 (<http://broadinstitute.github.io/picard>). The remaining reads were then assessed on  
731 the gene level using featureCounts from the Rsubread R-library (Liao et al., 2014)  
732 using the annotation information supplied by Gramene, release 5b+,  
733 ([http://ftp.gramene.org/maizesequence.org/release5b+/zea\\_mays.protein\\_coding.gff](http://ftp.gramene.org/maizesequence.org/release5b+/zea_mays.protein_coding.gff))  
734 . Gene annotation and ortholog information was retrieved from EnsemblPlants  
735 ([www.plants.ensembl.org](http://www.plants.ensembl.org)) via Biomart (Biomart<sup>7</sup>, release 29, *Z. mays* genes  
736 (AGPv3 (5b)), *A. thaliana* genes (2010-09-TAIR10) and *O. sativa japonica* genes  
737 (IRGSP-1.0), restricting the gene model to AGPv3 (5b) from EnsemblPlants.

738 (II) *Measurement of mRNA transcript abundance*: Transcripts per million (TPM) was  
739 used as a measure of mRNA abundance, which takes into account the length of the  
740 RNA transcripts and the sequencing depth (Wagner et al., 2012). Gene length was  
741 approximated by determining the sum of the exon lengths of the gene model. The  
742 TPMs were calculated for each gene in each sample. The median TPM value was  
743 calculated from three biological replicates for each cell type. An annotated list of  
744 genes with their expression levels at each developmental stage (cell type) and  
745 orthologs (based on Ensembl Compara from *A. thaliana* and *O. sativa*) was  
746 assembled (**Supplemental Data Set 1**).

747 (III) *Differential expression analysis and Venn diagrams*: Count data at the  
748 gene level were analyzed with DESeq2 (Love et al., 2014). All 15 cell-type-to-cell-  
749 type comparisons were performed and corrected for multiple testing over all genes  
750 and cell type comparisons using FDR (Benjamini and Hochberg, 1995)  
751 (**Supplemental Data Set 2**). Genes with a  $\log_2\text{FoldChange} > 1$  and  $\text{FDR} < 0.05$  (“padj”  
752 in supplemental tables) were considered significant differentially expressed, and  
753 Venn diagrams (R-library: `vennerable`; [https://r-forge.r-](https://r-forge.r-project.org/projects/vennerable)  
754 [project.org/projects/vennerable](https://r-forge.r-project.org/projects/vennerable)) were generated for certain comparisons (**Figure 4**).

755

## 756 **Expression profiles and pathway analysis**

757 Genes showing differential expression ( $\log_2\text{FoldChange}>1$  and  $\text{FDR}<0.05$ ) in at  
758 least one comparison were subjected to further analyses. To visualize gene  
759 expression values in heatmaps and to compare gene expression profiles during  
760 different stages of very early plant development, square root transformed TPM  
761 values were utilized. The median expression values were then transformed to  
762 standard units to follow the expression values of one gene across different  
763 developmental stages in the heatmaps. The dendrogram of the samples is based on  
764 Euclidean distances combined with hierarchical clustering with complete linkage. To  
765 classify genes into specific expression profiles, Pearson correlation analysis of the  
766 gene expression vector (square root transformed median TPM values as above)  
767 versus a binary vector encoding the different expression profiles, i.e., expressed only  
768 in egg cells and during fertilization (0,1,1,1,0,0)/(SP,EC,ZY12,ZY24,AC,BC) was  
769 performed (**Supplemental Data Set 1**). A stringent cutoff value of  $>0.9$  (Pearson  
770 correlation coefficient) was used to define a positive correlation with the respective  
771 profile.

772

## 773 **Comparison of gene expression levels in maize and rice gametes**

774 To compare the expression of the 80 most highly expressed genes from maize  
775 sperm and egg cells with their orthologs in rice (*Oryza sativa* ssp. *japonica*), data  
776 from Ensembl Compara (<http://plants.ensembl.org>, based on protein information for  
777 53 species) and the Rice Genome Annotation project (RGAP)  
778 ([http://rapdb.dna.affrc.go.jp/download/archive/RAP\\_MSU\\_2016-08-05.txt.gz](http://rapdb.dna.affrc.go.jp/download/archive/RAP_MSU_2016-08-05.txt.gz)) and  
779 orthologs from RGAP based on OrthoMCL were used (Li et al., 2003; Ouyang et al.,  
780 2007; Vilella et al., 2009). While OrthoMCL is based only on a comparison of protein  
781 sequences, Ensembl Compara also uses information from phylogenetic trees and  
782 therefore interprets sequence similarities based on the evolutionary development of  
783 a gene. Rice gene expression data (TPM) were obtained from Anderson et al.  
784 (2013). Maize and rice TPMs were square root transformed, and plastid transcripts  
785 were removed. Then, for each organism, the data were binned into 200 equally  
786 spaced expression categories, with the 99<sup>th</sup> percentile representing the maximum  
787 expression level. The color scale for the heatmaps shown in **Figure 2** represents the  
788 expression bin, indicating the relative expression level in the organism shown. For  
789 each maize gene, the respective rice orthologs in both resources were identified and

790 compared. If there were common orthologs predicted by both resources, these were  
791 chosen, and if not, all predictions were used. From this selected set of orthologs, the  
792 most highly expressed ortholog in rice was used for plotting. All orthologs are listed  
793 in **Supplemental Data Set 4**. In the heatmaps (**Figure 2**), the maximum of the color  
794 scale represents the 99<sup>th</sup> percentile, resulting in the same color for all maize genes  
795 shown (because all of the top 80 genes are within the most highly expressed 1% of  
796 the genes). Dark red bars in the rice column indicate that the gene was also in the  
797 top 1% most highly expressed genes in the rice data, and the lighter color indicates  
798 lower expression. Cyan lines represent expression levels as bar charts, with the  
799 dotted line indicating the median value of the column.

800

### 801 **Transcription factor gene list**

802 A list of potential TFs in maize based on conserved domains at the protein level was  
803 retrieved from Grassius (<http://grassius.org/tfomecollection.html>,  
804 [Maize\\_TFome\\_Bulk\\_data.txt](#)). A list of median expression values (TPM>1) of all TF  
805 genes, including their gene names and TF families, is shown in **Supplemental Data**  
806 **Set 7**. Important TF classes were identified by analyzing the fraction of expressed  
807 genes (TPM>1 in percent). Whenever the fraction of expressed genes of one cell  
808 type in one TF class exceeded the fractions in the other cell types, this class was  
809 discussed in the main text.

810

### 811 **Cell cycle gene list**

812 A list of cell cycle regulators identified in Arabidopsis (Vandepoele et al., 2002) was  
813 used to retrieve maize orthologs from the Rice Genome Annotation Project Database  
814 (University of Michigan), also comprising a full data set for maize (Kawahara et al.,  
815 2013) ([http://rice.plantbiology.msu.edu/annotation\\_pseudo\\_apk.shtml](http://rice.plantbiology.msu.edu/annotation_pseudo_apk.shtml)). Predicted  
816 cyclins (Hu et al., 2010) were added to the list, as well as genes reported to be  
817 involved in cell-cycle regulation in previous publications (Sauter et al., 1998;  
818 Dresselhaus et al., 1999b; Dresselhaus et al., 2006; Buendía-Monreal et al., 2011;  
819 Dante et al., 2014). Finally, the DNA replication-indicating genes encoding PCNA  
820 and MCM homologous proteins were added to the list manually based on Ensemble  
821 plants ([www.plants.ensembl.org](http://www.plants.ensembl.org)) (Sabelli et al., 2009). The genes were sorted into

822 different classes: CDKs and cyclins, followed by additional cell cycle-related factors  
823 (**Supplemental Data Set 3**).

824

### 825 **Auxin pathway analysis**

826 Information about auxin pathways was downloaded from  
827 ([http://www.genome.jp/dbget-bin/www\\_bget?ath04075](http://www.genome.jp/dbget-bin/www_bget?ath04075)). Maize genes in the different  
828 categories were obtained from the literature based on the gene list **Supplemental**  
829 **Data Set 3D** (important gene families). For each category (i.e., SAURs), all  
830 significantly ( $p$ -adjusted  $<0.05$ ) differentially expressed genes from the respective  
831 comparisons were selected. The median of the  $\log_2$ FoldChanges of these genes was  
832 calculated and represented by a color scale ranging from green (-2) to red (2). All  
833  $\log_2$ FoldChanges above or below these values were set to 2 (-2).

834

### 835 **Accession Numbers:**

836 The raw data (.fastq) plus supplemental tables, including count and TPM data for all  
837 replicates was uploaded to GEO and is available under accession number  
838 GSE98379. Gene identifiers are listed in Supplemental Data Set 1.

839

840

## 841 **SUPPLEMENTAL DATA**

842 **Supplemental Figure 1.** cDNA prepared from maize gametes/zygotes and initial  
843 validation based on the presence of selected transcripts.

844 **Supplemental Figure 2.** RNA-seq correlation plot and hierarchical clustering of  
845 maize gamete and zygote samples.

846 **Supplemental Figure 3.** Phylogenetic analysis of protein sequences of histone H3  
847 and H2A variants.

848 **Supplemental Table 1.** Summary of NGS runs, alignment process to Ensembl  
849 genome (AGPv3, ver: 82.6) and annotation to Ensembl genebuild (AGPv3\_5b,  
850 ver: 82.6).

851 **Supplemental Data Set 1.** Master table: binary identifier for venn diagram category  
852 membership. Median gene expression value (TPM, transcripts per million) of three  
853 biological replicates, for the indicated cell types, followed by genome coordinates,  
854 description, GO and InterPro annotation as well as information on homologous  
855 genes from Arabidopsis and rice.

856 **Supplemental Data Set 2.** List of differentially expressed genes for all 15 cell type  
857 comparisons, with  $\text{abs}(\log_2\text{FC}) > 1$  and p-adjusted  $< 0.05$ .

858 **Supplemental Data Set 3.** Lists of transcript levels of known genes required for  
859 fertilization and zygote development (see Figure 1B), expression profiles of  
860 transcription factors, cell cycle genes, and important gene families (see Figures 5,  
861 6, 7, and 8).

862 **Supplemental Data Set 4.** Lists of TOP80 maize sperm and egg cell genes  
863 compared to their predicted homologs/orthologs in rice gametes (see also Figure  
864 2).

865 **Supplemental Data Set 5.** Lists of 30 most highly expressed genes in maize sperm  
866 cell, egg cell, zygote 12HAP, zygote 24HAP, apical cell and basal cell,  
867 respectively (for detailed annotation see Suppl. Data Set 1).

868 **Supplemental Data Set 6.** Lists of gene expression profiles selected for Figure 4E.

869 **Supplemental Data Set 7.** List of expressed transcription factor classes (see also  
870 Figure 5A and B).

871 **Supplemental Data Set 8.** List of genes in the auxin pathway (see also Figure 7).

872

873

## 874 **ACKNOWLEDGMENTS**

875 We thank Thomas Stempfl and Christoph Möhle from the Kompetenzzentrum  
876 Fluoreszente Bioanalytik (KFB), a genomics core facility based at the University of  
877 Regensburg, for their support in optimizing the procedure used to generate libraries  
878 for Illumina sequencing from only a few plant cells. Funding through the Collaborate  
879 Research Center SFB960 of the German Research Foundation (DFG) to TD, JCE,  
880 and SS is gratefully acknowledged. The authors declare that they have no competing  
881 interests.

882

883

## 884 **AUTHOR CONTRIBUTIONS**

885 TD initiated and designed the project. JC, NGK, and PC performed wet lab  
886 experiments and interpreted results. JC, NS, SS, and JCE performed bioinformatics  
887 analyses. JC, NS, and TD wrote the manuscript with input from all authors.

888

889

890 **FIGURE LEGENDS**

891 **Figure 1. Time course of zygote development and validation of RNA-Seq data.**

892 (A) Sperm cells. (B) Egg cell. (C) Zygote at 24 hours after pollination (HAP). (D)  
893 Zygote at 30 HAP at anaphase. (E) Zygote at 35 HAP at telophase. Arrowheads  
894 indicate phragmoplast between daughter chromosome sets. (F) Zygote at 43 HAP  
895 during asymmetric cell division (ACD). (G) Zygote at 48 HAP. Cytokinesis is  
896 completed. Dotted line indicates the cell division plane. (H) Apical (AC) and basal  
897 cell (BC) have been separated at 54 HAP. Bright field microscopy images are shown  
898 on the left and UV images of DAPI stained cells on the right. Scale bars: 10  $\mu$ m. (I)  
899 Validation of RNA-Seq data with known genes, as indicated. Top row: Genes  
900 preferentially expressed in sperm cells; middle row: Genes highly expressed in egg  
901 cells and downregulated after fertilization; bottom row: Expression of cell cycle  
902 regulators. Transcript levels are shown as TPM (transcripts per million) values  
903 (means  $\pm$  SD) of three biological replicates.

904

905 **Figure 2. Heatmap showing a comparison of the 80 most highly expressed**  
906 **genes in maize gametes and their predicted orthologs in the corresponding**

907 **rice gametes.** (A) TOP80 most highly expressed genes in maize sperm cells and  
908 (B) TOP80 genes in maize egg cells. Note that all maize genes display a TPM>200  
909 and are thus indicated by red bars. For better visualization, rice and maize gene  
910 expression values (TPM) were square root transformed and classified into 80  
911 expression categories using the 99<sup>th</sup> percentile of the data to summarize all higher  
912 expression values. Plastid genomes were excluded, as they showed overshooting of  
913 expression in the rice data. Non-expressed genes in the rice data and genes lacking  
914 a clear homolog are marked by black bars. Orthologous gene information is based  
915 on the EnsemblPlants Compara database, The Rice Genome Annotation Project  
916 (RGAP), and orthologs from RGAP based on OrthoMCL. Maize genes encoding  
917 histones and high-mobility group genes are shaded in purple, proteins involved in  
918 translation are in green, and EA1-box proteins and predicted secreted CRPs are in  
919 yellow. Proteins were classified according to InterPro.

920

921 **Figure 3. Expression of major chromatin structure protein genes in maize**  
922 **gametes, zygotes, and daughter cells.** (A) Histone H1, (B) histone H3, (C) histone

923 H4, (D) histone H2A, (E) histone H2B, and (F) high mobility group protein Hmgd1. All  
924 significantly expressed genes of the various gene families are presented. See  
925 Supplemental Figure 3 for phylogenetic analysis of male-specific and active  
926 chromatin-specific variants of histones H3 and H2A. Gene identifiers are listed in  
927 Supplemental Data Set 7 (important gene families). Transcript levels in the cells  
928 indicated are given as TPM values (means  $\pm$  SD).

929

930 **Figure 4. Gene expression dynamics in maize gametes, zygotes, and two-**  
931 **celled pro-embryo cells.** Genes with a  $\text{abs}(\log_2\text{FC}) > 1$  and  $p\text{-adjusted} < 0.05$  were  
932 considered to be biologically meaningful. (A) Comparison of the number of genes  
933 induced in sperm cells (SP) and egg cells (EC) versus zygotes at 12 HAP (Zy12). (B)  
934 Comparisons of genes upregulated in zygotes at 12 HAP versus sperm and egg  
935 cells. (C) Number of genes induced in zygotes at 24 HAP compared to apical (AC)  
936 and basal (BC) cells. (D) Comparison of genes upregulated in apical and basal cells  
937 versus zygotes at 24 HAP (Zy24). (E) Selected gene expression profiles across the  
938 specific cell types analyzed (see Supplemental Data Set 6). The Pearson correlation  
939 ( $> 0.9$ ) of square root transformed TPM values per gene and binary profile vectors  
940 were used to identify genes belonging to a specific profile. The total number of genes  
941 including TFs contained in each profile is shown at the bottom. The mean expression  
942 level of all genes per specific cell type is plotted in each profile (black line). (F) Table  
943 of differentially upregulated genes ( $\log_2\text{FC} > 1$ ,  $p\text{-adjusted} < 0.05$ ) of row cell type  
944 versus column cell type. The last column show the number of differentially  
945 upregulated genes in a row cell type versus all other cell types.

946

947 **Figure 5. Expression levels of transcription factor (TF) and MAB genes in**  
948 **gametes, zygotes, and early two-celled pro-embryo cells in maize.** (A)  
949 Expression levels of TF genes in gametes and at early developmental stages after  
950 fertilization. Genes with  $\text{abs}(\log_2\text{FC}) > 1$  and  $p\text{-adjusted} < 0.05$  in at least one cell type  
951 comparison were considered. To make the expression levels comparable across  
952 multiple cell types, z-scores were calculated from the square root transformed TPM  
953 values corresponding to the number of standard deviations between the cell type-  
954 specific expression value and the mean expression value of the respective gene.  
955 Genes were ordered by TF classes (black/blue bars). Black and blue fonts were  
956 used alternatively to distinguish the various classes. See Supplemental Data Sets 2

957 and 7 for details. **(B)** Expression analysis of selected maize genes encoding  
958 homologs of Arabidopsis early embryogenesis-related TFs as well as **(C)** MATH-BTB  
959 (MAB) family genes involved in ACD.

960

961 **Figure 6. Gene expression analysis of cell cycle regulators.** **(A)** Major regulators  
962 of the maize cell cycle (Supplemental Data Set 2). Transformation of gene  
963 expression values as described above. Genes were ordered into protein classes  
964 based on data from the literature (see Methods for details). **(B)** Summary of the time  
965 course of pollen tube (PT) growth, fertilization, and zygote development. Cell cycle  
966 stages of the selected cells are indicated based on the currently reported expression  
967 data.

968

969 **Figure 7. Analysis of the auxin pathway in gametes, zygotes, and during early**  
970 **embryogenesis.** **(A)** Expression analysis of the most highly expressed auxin  
971 biosynthesis, transport, and auxin response-related genes. **(B)** Auxin pathway  
972 analysis using three developmental transitions during zygote development. The  
973 median values over the  $\log_2$ FoldChanges of all differentially expressed genes ( $p$ -  
974 adjusted  $<0.05$ ) from the respective comparison are color-coded in green  
975 (downregulated) and red (upregulated). All  $\log_2$ FoldChanges above 2 or below  $-2$   
976 were set to  $2/-2$  to improve visualization. *White boxes*: no significant  $\log_2$ FC found,  
977 *+u*: ubiquitination, *blue line*: inhibition, *dotted gray line*: dissociation, *red dashed line*:  
978 expression. Gene pathway based on KEGG analysis. See Supplemental Data Set 2  
979 for genes.

980

981 **Figure 8. Expression analysis of selected maize genes with putative roles in**  
982 **signaling during gamete interaction and early embryogenesis.** **(A)**  $\text{Ca}^{2+}$ -  
983 dependent phospholipid-binding annexin family proteins, **(B)** sperm-specific  
984 receptor-like kinases, and **(C)** fertilization-regulated receptor-like kinases. Gene  
985 identifiers are listed in Supplemental Data Set 2 (important gene families). Transcript  
986 levels in the cells indicated are given as TPM values (means  $\pm$  SD).

987

988

989

990 **Table 1.** Summary of samples, NGS runs, alignment to the Ensembl genome  
 991 (AGPv3, ver. 82.6), and annotation to Ensembl genebuild (AGPv3\_5b, ver. 82.6).  
 992 The number of genes expressed in at least two of three replicates are given. See  
 993 Supplemental Table 1 for details.

994  
 995

Sample	Cell number per replicate	All reads after trimming	Aligned pairs mapped unique	% Mapped reads per trimmed reads	Expressed genes (TPM>1)
Sperm Cell1	~1,000	68,988,450	26,514,492	77	<b>11,819</b>
Sperm Cell2	~1,000	102,929,736	38,689,716	75	
Sperm Cell3	~1,000	86,448,904	33,271,851	77	
Egg Cell1	20	57,338,078	13,901,359	48	<b>16,026</b>
Egg Cell2	20	63,488,722	22,978,462	72	
Egg Cell3	20	69,199,124	25,147,141	73	
Zygote_12HAP1	14	70,632,412	15,761,484	45	<b>19,865</b>
Zygote_12HAP2	15	76,840,694	19,297,245	50	
Zygote_12HAP3	15	55,130,854	11,323,005	41	
Zygote_24HAP1	16	82,825,752	20,424,191	49	<b>19,171</b>
Zygote_24HAP2	16	80,911,418	20,173,448	50	
Zygote_24HAP3	17	87,134,202	19,443,455	45	
Apical Cell1	16	94,779,064	29,713,124	63	<b>17,747</b>
Apical Cell2	16	68,636,668	20,927,946	61	
Apical Cell3	16	74,074,566	23,422,549	63	
Basal Cell1	13	71,456,410	22,440,462	63	<b>18,069</b>
Basal Cell2	13	68,963,988	21,238,495	62	
Basal Cell3	14	67,950,552	20,886,111	61	

996  
 997

998

999

1000

1001 **REFERENCES**

1002 **Ahmad, K., and Henikoff, S.** (2002). The histone variant H3.3 marks active  
 1003 chromatin by replication-independent nucleosome assembly. *Mol Cell* **9**, 1191-  
 1004 1200.

1005 **Am, B., Lohse, M., and Usadel, B.** (2014). Trimmomatic: a flexible trimmer for  
 1006 Illumina sequence data. *Bioinformatics* **30**, 2114-2120.

1007 **Amien, S., Kliwer, I., Marton, M.L., Debener, T., Geiger, D., Becker, D., and**  
 1008 **Dresselhaus, T.** (2010). Defensin-like ZmES4 mediates pollen tube burst in  
 1009 maize via opening of the potassium channel KZM1. *PLoS Biol* **8**, e1000388.

1010 **Anderson, S.N., Johnson, C.S., Jones, D.S., Conrad, L.J., Gou, X., Russell,**  
1011 **S.D., and Sundaresan, V.** (2013). Transcriptomes of isolated *Oryza sativa*  
1012 gametes characterized by deep sequencing: evidence for distinct sex-dependent  
1013 chromatin and epigenetic states before fertilization. *Plant J* **76**, 729-741.

1014 Autran, D., Baroux, C., Raissig, M.T., Lenormand, T., Wittig, M., Grob, S., Steimer,  
1015 A., Barann, M., Klostermeier, U.C., Leblanc, O., Vielle-Calzada, J.P., Rosenstiel,  
1016 P., Grimanelli, D., Grossniklaus, U. (2011). Maternal epigenetic pathways control  
1017 parental contributions to Arabidopsis early embryogenesis. *Cell* **27**,707-719.

1018 **Baroux, C., and Grossniklaus, U.** (2015). The maternal-to-zygotic transition in  
1019 flowering plants: Evidence, mechanisms, and plasticity. *Curr Top Dev Biol* **113**,  
1020 351-371.

1021 **Benjamini, Y., and Hochberg, Y.** (1995). Controlling the false discovery rate: a  
1022 practical and powerful approach to multiple testing. *J Royal Statist Soc Ser B* **57**,  
1023 289–300.

1024 **Borges, F., Gomes, G., Gardner, R., Moreno, N., McCormick, S., Feijo, J.A., and**  
1025 **Becker, J.D.** (2008). Comparative transcriptomics of Arabidopsis sperm cells.  
1026 *Plant Physiol* **148**, 1168-1181.

1027 **Boutilier, K., Offringa, R., Sharma, V.K., Kieft, H., Ouellet, T., Zhang, L., Hattori,**  
1028 **J., Liu, C.-M., van Lammeren, A.A.M., Miki, B.L.A., Custers, J.B.M., and van**  
1029 **Lookeren Campagne, M.M.** (2002). Ectopic expression of BABY BOOM triggers  
1030 a conversion from vegetative to embryonic growth. *Plant Cell* **14**, 1737-1749.

1031 **Breuninger, H., Rikirsch, E., Hermann, M., Ueda, M., and Laux, T.** (2008).  
1032 Differential expression of *WOX* genes mediates apical-basal axis formation in  
1033 the Arabidopsis embryo. *Dev Cell* **14**, 867-876.

1034 **Budkevich, T.V., Timchenko, A.A., Tiktopulo, E.I., Negrutskii, B.S., Shalak, V.F.,**  
1035 **Petrushenko, Z.M., Aksenov, V.L., Willumeit, R., Kohlbrecher, J., Serdyuk,**  
1036 **I.N., and El'skaya, A.V.** (2002). Extended conformation of mammalian  
1037 translation elongation factor 1A in solution. *Biochemistry* **41**, 15342-15349.

1038 **Buendía-Monreal, M., Rentería-Canett, I., Guerrero-Andrade, O., Bravo-Alberto,**  
1039 **C.E., Martínez-Castilla, L.P., García, E., and Vázquez-Ramos, J.M.** (2011).  
1040 The family of maize D-type cyclins: genomic organization, phylogeny and  
1041 expression patterns. *Physiol Plantarum* **143**, 297-308.

1042 **Chen, J., Lausser, A., and Dresselhaus, T.** (2014). Hormonal responses during  
1043 early embryogenesis in maize. *Biochem Soc Transact* **42**, 325-331.

1044 **Chen, J., Gutjahr, C., Bleckmann, A., and Dresselhaus, T.** (2015). Calcium  
1045 signaling during reproduction and biotrophic fungal interactions in plants. *Mol*  
1046 *Plant* **8**, 595-611.

1047 **Chettoor, A.M., Givan, S.A., Cole, R.A., Coker, C.T., Unger-Wallace, E.,**  
1048 **Vejlupkova, Z., Vollbrecht, E., Fowler, J.E., Evans, M.M.** (2014). Discovery of  
1049 novel transcripts and gametophytic functions via RNA-seq analysis of maize  
1050 gametophytic transcriptomes. *Genome Biol* **15**, 414.

1051 **Chevalier, F., Perazza, D., Laporte, F., Le Hénanff, G., Hornitschek, P.,**  
1052 **Bonneville, J.-M., Herzog, M., and Vachon, G.** (2008). GeBP and GeBP-like  
1053 proteins are noncanonical leucine-zipper transcription factors that regulate  
1054 cytokinin response in Arabidopsis. *Plant Physiol* **146**, 1142-1154.

1055 **Cordts, S., Bantin, J., Wittich, P.E., Kranz, E., Lörz, H., and Dresselhaus, T.**  
1056 (2001). ZmES genes encode peptides with structural homology to defensins and  
1057 are specifically expressed in the female gametophyte of maize. *Plant J* **25**, 103-  
1058 114.

1059 **Cui, Y., Dinman, J.D., Kinzy, T.G., and Peltz, S.W.** (1998). The Mof2/Sui1 protein  
1060 is a general monitor of translational accuracy. *Mol Cell Biol* **18**, 1506-1516.

1061 **Dante, R.A., Larkins, B.A., and Sabelli, P.A.** (2014). Cell cycle control and seed  
1062 development. *Front Plant Sci* **5**, 493.

1063 **Deal, R.B., and Henikoff, S.** (2011). Histone variants and modifications in plant  
1064 gene regulation. *Curr Opin Plant Biol* **14**, 116-122.

1065 **Del Toro-De León, G., García-Aguilar, M., and Gillmor, C.S.** (2014). Non-  
1066 equivalent contributions of maternal and paternal genomes to early plant  
1067 embryogenesis. *Nature* **514**, 624-627.

1068 **Dobin, A., Davis, C.A., Schlesinger, F., Drenkow, J., Zaleski, C., Jha, S., Batut,**  
1069 **P., Chaisson, M., and Gingeras, T.R.** (2013). STAR: Ultrafast universal RNA-  
1070 Seq aligner. *Bioinformatics* **29**, 15–21.

1071 **Dresselhaus, T., Cordts, S., and Lörz, H.** (1999a). A transcript encoding translation  
1072 initiation factor eIF-5A is stored in unfertilized egg cells of maize. *Plant Mol Biol*  
1073 **39**, 1063-1071.

1074 **Dresselhaus, T., Lausser, A., and Márton, M.L.** (2011). Using maize as a model to  
1075 study pollen tube growth and guidance, cross-incompatibility and sperm delivery  
1076 in grasses. *Annals Bot* **108**, 727-737.

- 1077 **Dresselhaus, T., Sprunck, S., and Wessel, G.M.** (2016). Fertilization mechanisms  
1078 in flowering plants. *Curr Biol* **26**, R125-139.
- 1079 **Dresselhaus, T., Srilunchang, K.-O., Leljak-Levanic, D., Schreiber, D.N., and**  
1080 **Garg, P.** (2006). The fertilization-induced DNA replication factor MCM6 of maize  
1081 shuttles between cytoplasm and nucleus, and is essential for plant growth and  
1082 development. *Plant Physiol* **140**, 512-527.
- 1083 **Dresselhaus, T., Cordts, S., Heuer, S., Sauter, M., Lörz, H., and Kranz, E.**  
1084 (1999b). Novel ribosomal genes from maize are differentially expressed in the  
1085 zygotic and somatic cell cycles. *Mol Gen Genet* **261**, 416-427.
- 1086 **Dupuis, I., Roeckel, P., Matthys-Rochon, E., and Dumas, C.** (1987). Procedure to  
1087 isolate viable sperm cells from corn (*Zea mays* L.) pollen grains. *Plant Physiol*  
1088 **85**, 876-878.
- 1089 **Engel, M.L., Chaboud, A., Dumas, C., and McCormick, S.** (2003). Sperm cells of  
1090 *Zea mays* have a complex complement of mRNAs. *Plant J* **34**, 697-707.
- 1091 **Friml, J., Vieten, A., Sauer, M., Weijers, D., Schwarz, H., Hamann, T., Offringa,**  
1092 **R., and Jurgens, G.** (2003). Efflux-dependent auxin gradients establish the  
1093 apical-basal axis of Arabidopsis. *Nature* **426**, 147-153.
- 1094 **Gerke, V., Creutz, C.E., and Moss, S.E.** (2005). Annexins: linking Ca<sup>2+</sup> signalling to  
1095 membrane dynamics. *Nat Rev Mol Cell Biol* **6**, 449-461.
- 1096 **Grimanelli, D., Perotti, E., Ramirez, J., and Leblanc, O.** (2005) Timing of the  
1097 maternal-to-zygotic transition during early seed development in maize. *Plant Cell*  
1098 **17**, 1061-1072.
- 1099 **Guo, S., and Kemphues, K.J.** (1995). *par-1*, a gene required for establishing  
1100 polarity in *C. elegans* embryos, encodes a putative Ser/Thr kinase that is  
1101 asymmetrically distributed. *Cell* **81**, 611-620.
- 1102 **Hecht, V., Vielle-Calzada, J.-P., Hartog, M.V., Schmidt, E.D.L., Boutilier, K.,**  
1103 **Grossniklaus, U., and de Vries, S.C.** (2001). The Arabidopsis somatic  
1104 embryogenesis receptor kinase 1 gene is expressed in developing ovules and  
1105 embryos and enhances embryogenic competence in culture. *Plant Physiol* **127**,  
1106 803-816.
- 1107 **Hu, X., Cheng, X., Jiang, H., Zhu, S., Cheng, B., and Xiang, Y.** (2010). Genome-  
1108 wide analysis of cyclins in maize (*Zea mays*). *Genet Mol Res* **9**, 1490-1503.
- 1109 **Ingouff, M., Rademacher, S., Holec, S., Šoljić, L., Xin, N., Readshaw, A., Foo,**  
1110 **S.H., Lahouze, B., Sprunck, S., and Berger, F.** (2010). Zygotic resetting of the

1111 HISTONE 3 variant repertoire participates in epigenetic reprogramming in  
1112 Arabidopsis. *Curr Biol* **20**, 2137-2143.

1113 **Juranić, M., Srilunchang, K.-o., Krohn, N.G., Leljak-Levanić, D., Sprunck, S.,**  
1114 **and Dresselhaus, T.** (2012). Germline-specific MATH-BTB substrate adaptor  
1115 MAB1 regulates spindle length and nuclei identity in maize. *Plant Cell* **24**, 4974-  
1116 4991.

1117 **Kawahara, Y., La Bastide, M., Hamilton, J.P., Kanamori, H., McCombie, W.R.,**  
1118 **Ouyang, S., Schwartz, D.C., Tanaka, T., Wu, J., Zhou, S., Childs, K.L.,**  
1119 **Davidson, R.M., Lin, H., Quesada-Ocampo, L., Vaillancourt, B., Sakai, H.,**  
1120 **Lee, S.S., Kim, J., Numa, H., Itoh, T., Buell, C.R., and Matsumoto, T.** (2013).  
1121 Improvement of the *Oryza sativa* Nipponbare reference genome using next  
1122 generation sequence and optical map data. *Rice* **6**, 4.

1123 **Kim, D., Pertea, G., Trapnell, C., Pimentel, H., Kelley, R., and Salzberg, S.L.**  
1124 (2013). TopHat2: accurate alignment of transcriptomes in the presence of  
1125 insertions, deletions and gene fusions. *Genome Biol* **14**, R36.

1126 **Kleine, T.** (2012). *Arabidopsis thaliana* mTERF proteins: evolution and functional  
1127 classification. *Front Plant Sci* **3**, 233.

1128 **Kranz, E., Bautor, J., and Lorz, H.** (1991). *In vitro* fertilization of single, isolated  
1129 gametes of maize mediated by electrofusion. *Sex Plant Reprod* **4**, 12-16.

1130 **Lee, M.T., Bonneau, A.R., and Giraldez, A.J.** (2014). Zygotic genome activation  
1131 during the maternal-to-zygotic transition. *Annu Rev Cell Dev Biol* **30**, 581-613.

1132 **Lehti-Shiu, M.D., Adamczyk, B.J., and Fernandez, D.E.** (2005). Expression of  
1133 MADS-box genes during the embryonic phase in Arabidopsis. *Plant Mol Biol* **58**,  
1134 89-107.

1135 **Li, L., Stoeckert, C.J., Jr., and Roos, D.S.** (2003). OrthoMCL: identification of  
1136 ortholog groups for eukaryotic genomes. *Genome Res* **13**, 2178-2189.

1137 **Liao, Y., Smyth, G.K., and Shi, W.** (2014). featureCounts: an efficient general  
1138 purpose program for assigning sequence reads to genomic features.  
1139 *Bioinformatics* **30**, 923-930.

1140 **Long, R.M., Singer, R.H., Meng, X., Gonzalez, I., Nasmyth, K., and Jansen, R.P.**  
1141 (1997). Mating type switching in yeast controlled by asymmetric localization of  
1142 ASH1 mRNA. *Science* **277**, 383-387.

1143 **Lotan, T., Ohto, M., Yee, K.M., West, M.A., Lo, R., Kwong, R.W., Yamagishi, K.,**  
1144 **Fischer, R.L., Goldberg, R.B., and Harada, J.J.** (1998). Arabidopsis LEAFY

1145 COTYLEDON1 is sufficient to induce embryo development in vegetative cells.  
1146 Cell **93**, 1195-1205.

1147 **Love, M.I., Huber, W., and Anders, S.** (2014). Moderated estimation of fold change  
1148 and dispersion for RNA-seq data with DESeq2. Genome Biol **15**, 550.

1149 **Lowe, K., Wu, E., Wang, N., Hoerster, G., Hastings, C., Cho, M.J., Scelonge, C.,**  
1150 **Lenderts, B., Chamberlin, M., Cushatt, J., Wang, L., Ryan, L., Khan, T.,**  
1151 **Chow-Yiu, J., Hua, W., Yu, M., Banh, J., Bao, Z., Brink, K., Igo, E., Rudrappa,**  
1152 **B., Shamseer, P.M., Bruce, W., Newman, L., Shen, B., Zheng, P., Bidney, D.,**  
1153 **Falco, S.C., Register, I.J., Zhao, Z.Y., Xu, D., Jones, T.J., and Gordon-**  
1154 **Kamm, W.J.** (2016). Morphogenic regulators Baby Boom and Wuschel improve  
1155 monocot transformation. Plant Cell **28**, 1998-2015.

1156 **Maiorano, D., Lutzmann, M., and Mechali, M.** (2006). MCM proteins and DNA  
1157 replication. Curr Opin Cell Biol **18**, 130-136.

1158 **Martin, M.** (2011). Cutadapt removes adapter sequences from high-throughput  
1159 sequencing reads. EMBnet J **17**, 10-12.

1160 **Márton, M.L., Cordts, S., Broadhvest, J., and Dresselhaus, T.** (2005). Micropylar  
1161 pollen tube guidance by egg apparatus 1 of maize. Science **307**, 573-576.

1162 **Meijer, M., and Murray, J.A.** (2001). Cell cycle controls and the development of  
1163 plant form. Curr Opin Plant Biol **4**, 44-49.

1164 **Mitsuda, N., Isono, T., and Sato, M.H.** (2003). Arabidopsis CAMTA family proteins  
1165 enhance V-PPase expression in pollen. Plant Cell Physiol **44**, 975-981.

1166 **Nodine, M.D., and Bartel, D.P.** (2012). Maternal and paternal genomes contribute  
1167 equally to the transcriptome of early plant embryos. Nature **482**, 94–97.

1168 **Okada, T., Endo, M., Singh, M.B., and Bhalla, P.L.** (2005). Analysis of the histone  
1169 H3 gene family in Arabidopsis and identification of the male-gamete-specific  
1170 variant AtMGH3. Plant J **44**, 557-568.

1171 **Ouyang, S., Zhu, W., Hamilton, J., Lin, H., Campbell, M., Childs, K., Thibaud-**  
1172 **Nissen, F., Malek, R.L., Lee, Y., Zheng, L., Orvis, J., Haas, B., Wortman, J.,**  
1173 **and Buell, C.R.** (2007). The TIGR rice genome annotation resource:  
1174 improvements and new features. Nucl Acids Res **35**, D883-887.

1175 **Ouyang, X., Li, J., Li, G., Li, B., Chen, B., Shen, H., Huang, X., Mo, X., Wan, X.,**  
1176 **Lin, R., Li, S., Wang, H., and Deng, X.W.** (2011). Genome-wide binding site  
1177 analysis of FAR-RED ELONGATED HYPOCOTYL3 reveals its novel function in  
1178 Arabidopsis development. Plant Cell **23**, 2514-2535.

1179 **Petrášek, J., and Friml, J.** (2009). Auxin transport routes in plant development.  
1180 *Development* **136**, 2675-2688.

1181 **Pintard, L., Willis, J.H., Willems, A., Johnson, J.-L.F., Srayko, M., Kurz, T.,**  
1182 **Glaser, S., Mains, P.E., Tyers, M., Bowerman, B., and Peter, M.** (2003). The  
1183 BTB protein MEL-26 is a substrate-specific adaptor of the CUL-3 ubiquitin-ligase.  
1184 *Nature* **425**, 311-316.

1185 **Ren, H., and Gray, W.M.** (2015). SAUR proteins as effectors of hormonal and  
1186 environmental signals in plant growth. *Mol Plant* **8**, 1153-1164.

1187 **Rieseberg, L.H., and Willis, J.H.** (2007). Plant speciation. *Science* **317**, 910-914.

1188 **Russell, S.D., Gou, X., Wong, C.E., Wang, X., Yuan, T., Wei, X., Bhalla, P.L., and**  
1189 **Singh, M.B.** (2012a). Genomic profiling of rice sperm cell transcripts reveals  
1190 conserved and distinct elements in the flowering plant male germ lineage. *New*  
1191 *Phytol* **195**, 560-573.

1192 **Russell, S.D., Gou, X., Wong, C.E., Wang, X., Yuan, T., Wei, X., Bhalla, P.L., and**  
1193 **Singh, M.B.** (2012b). Genomic profiling of rice sperm cell transcripts reveals  
1194 conserved and distinct elements in the flowering plant male germ lineage. *New*  
1195 *Phytol* **195**, 560-573.

1196 **Sabelli, P.A., Hoerster, G., Lizarraga, L.E., Brown, S.W., Gordon-Kamm, W.J.,**  
1197 **and Larkins, B.A.** (2009). Positive regulation of minichromosome maintenance  
1198 gene expression, DNA replication, and cell transformation by a plant  
1199 retinoblastoma gene. *Proc Natl Acad Sci USA* **106**, 4042-4047.

1200 **Sabelli, P.A., Liu, Y., Dante, R.A., Lizarraga, L.E., Nguyen, H.N., Brown, S.W.,**  
1201 **Klingler, J.P., Yu, J., LaBrant, E., Layton, T.M., Feldman, M., and Larkins,**  
1202 **B.A.** (2013). Control of cell proliferation, endoreduplication, cell size, and cell  
1203 death by the retinoblastoma-related pathway in maize endosperm. *Proc Natl*  
1204 *Acad Sci USA* **110**, E1827-1836.

1205 **Salvo, S.A.G.D., Hirsch, C.N., Buell, C.R., Kaeppler, S.M., and Kaeppler, H.F.**  
1206 (2014). Whole transcriptome profiling of maize during early somatic  
1207 embryogenesis reveals altered expression of stress factors and embryogenesis-  
1208 related genes. *PLoS ONE* **9**, e111407.

1209 **Sauter, M., von Wieggen, P., Lörz, H., and Kranz, E.** (1998). Cell cycle regulatory  
1210 genes from maize are differentially controlled during fertilization and first  
1211 embryonic cell division. *Sex Plant Reprod* **11**, 41-48.

1212 **Schier, A.F.** (2007). The maternal-zygotic transition: Death and birth of RNAs.  
1213 *Science* **316**, 406-407.

1214 **Schnable, P.S., Ware, D., Fulton, R.S., Stein, J.C., Wei, F., Pasternak, S., Liang,**  
1215 **C., Zhang, J., Fulton, L., Graves, T.A., Minx, P., Reily, A.D., Courtney, L.,**  
1216 **Kruchowski, S.S., Tomlinson, C., Strong, C., Delehaunty, K., Fronick, C.,**  
1217 **Courtney, B., Rock, S.M., Belter, E., Du, F., Kim, K., Abbott, R.M., Cotton,**  
1218 **M., Levy, A., Marchetto, P., Ochoa, K., Jackson, S.M., Gillam, B., Chen, W.,**  
1219 **Yan, L., Higginbotham, J., Cardenas, M., Waligorski, J., Applebaum, E.,**  
1220 **Phelps, L., Falcone, J., Kanchi, K., Thane, T., Scimone, A., Thane, N.,**  
1221 **Henke, J., Wang, T., Ruppert, J., Shah, N., Rotter, K., Hodges, J.,**  
1222 **Ingenthron, E., Cordes, M., Kohlberg, S., Sgro, J., Delgado, B., Mead, K.,**  
1223 **Chinwalla, A., Leonard, S., Crouse, K., Collura, K., Kudrna, D., Currie, J.,**  
1224 **He, R., Angelova, A., Rajasekar, S., Mueller, T., Lomeli, R., Scara, G., Ko, A.,**  
1225 **Delaney, K., Wissotski, M., Lopez, G., Campos, D., Braidotti, M., Ashley, E.,**  
1226 **Golser, W., Kim, H., Lee, S., Lin, J., Dujmic, Z., Kim, W., Talag, J., Zuccolo,**  
1227 **A., Fan, C., Sebastian, A., Kramer, M., Spiegel, L., Nascimento, L., Zutavern,**  
1228 **T., Miller, B., Ambroise, C., Muller, S., Spooner, W., Narechania, A., Ren, L.,**  
1229 **Wei, S., Kumari, S., Faga, B., Levy, M.J., McMahan, L., Van Buren, P.,**  
1230 **Vaughn, M.W., Ying, K., Yeh, C.T., Emrich, S.J., Jia, Y., Kalyanaraman, A.,**  
1231 **Hsia, A.P., Barbazuk, W.B., Baucom, R.S., Brutnell, T.P., Carpita, N.C.,**  
1232 **Chaparro, C., Chia, J.M., Deragon, J.M., Estill, J.C., Fu, Y., Jeddelloh, J.A.,**  
1233 **Han, Y., Lee, H., Li, P., Lisch, D.R., Liu, S., Liu, Z., Nagel, D.H., McCann,**  
1234 **M.C., SanMiguel, P., Myers, A.M., Nettleton, D., Nguyen, J., Penning, B.W.,**  
1235 **Ponnala, L., Schneider, K.L., Schwartz, D.C., Sharma, A., Soderlund, C.,**  
1236 **Springer, N.M., Sun, Q., Wang, H., Waterman, M., Westerman, R.,**  
1237 **Wolfgruber, T.K., Yang, L., Yu, Y., Zhang, L., Zhou, S., Zhu, Q., Bennetzen,**  
1238 **J.L., Dawe, R.K., Jiang, J., Jiang, N., Presting, G.G., Wessler, S.R., Aluru, S.,**  
1239 **Martienssen, R.A., Clifton, S.W., McCombie, W.R., Wing, R.A., and Wilson,**  
1240 **R.K.** (2009). The B73 maize genome: complexity, diversity, and dynamics.  
1241 *Science* **326**, 1112-1115.

1242 **Schon, M.A., and Nodine, M.D.** (2017). Widespread contamination of Arabidopsis  
1243 embryo and endosperm transcriptome data sets. *Plant Cell* **29**, 608-617.

1244 **Schreiber, D.N., Bantin, J., and Dresselhaus, T.** (2004). The MADS box  
1245 transcription factor ZmMADS2 is required for anther and pollen maturation in

1246 maize and accumulates in apoptotic bodies during anther dehiscence. *Plant*  
1247 *Physiol* **134**, 1069-1079.

1248 **Siller, K.H., and Doe, C.Q.** (2009). Spindle orientation during asymmetric cell  
1249 division. *Nat Cell Biol* **11**, 365-374.

1250 **Thomas, J.O., and Travers, A.A.** (2001). HMG1 and 2, and related 'architectural'  
1251 DNA-binding proteins. *Trends Biochem Sci* **26**, 167-174.

1252 **Tuteja, N., Tran, N., Dang, H., and Tuteja, R.** (2011). Plant MCM proteins: role in  
1253 DNA replication and beyond. *Plant Mol Biol* **77**, 537-545.

1254 **Uebler, S., Márton, M.L., and Dresselhaus, T.** (2015). Classification of EA1-box  
1255 proteins and new insights into their role during reproduction in grasses. *Plant*  
1256 *Reprod* **28**, 183-197.

1257 **Vandepoele, K., Raes, J., Veylder, L., Rouzé, P., Rombauts, S., and Inzé, D.**  
1258 (2002). Genome-wide analysis of core cell cycle genes in *Arabidopsis*. *Plant Cell*  
1259 **14**, 903-916.

1260 **Vilella, A.J., Severin, J., Ureta-Vidal, A., Heng, L., Durbin, R., and Birney, E.**  
1261 (2009). EnsemblCompara GeneTrees: Complete, duplication-aware  
1262 phylogenetic trees in vertebrates. *Genome Res* **19**, 327-335.

1263 **Wagner, G.P., Kin, K., and Lynch, V.J.** (2012). Measurement of mRNA abundance  
1264 using RNA-seq data: RPKM measure is inconsistent among samples. *Theory*  
1265 *Biosci* **131**, 281-285.

1266 **Wei, K., Chen, J., Wang, Y., Chen, Y., Chen, S., Lin, Y., Pan, S., Zhong, X., and**  
1267 **Xie, D.** (2012). Genome-wide analysis of bZIP-encoding genes in maize. *DNA*  
1268 *Res* **19**, 463-476.

1269 **Wu, R.-C., Jiang, M., Beaudet, A.L., and Wu, M.-Y.** (2013). ARID4A and ARID4B  
1270 regulate male fertility, a functional link to the AR and RB pathways. *Proc Natl*  
1271 *Acad Sci USA* **110**, 4616-4621.

1272 **Wuest, S.E., Vijverberg, K., Schmidt, A., Weiss, M., Gheyselinck, J., Lohr, M.,**  
1273 **Wellmer, F., Rahnenfuhrer, J., von Mering, C., and Grossniklaus, U.** (2010).  
1274 *Arabidopsis* female gametophyte gene expression map reveals similarities  
1275 between plant and animal gametes. *Curr Biol* **20**, 506-512.

1276 **Yue, R., Tie, S., Sun, T., Zhang, L., Yang, Y., Qi, J., Yan, S., Han, X., Wang, H.,**  
1277 **and Shen, C.** (2015). Genome-wide identification and expression profiling  
1278 analysis of *ZmPIN*, *ZmPILS*, *ZmLAX* and *ZmABCB* auxin transporter gene

1279 families in maize (*Zea mays* L.) under various abiotic stresses. PLoS One **10**,  
1280 e0118751.

1281 **Zhang, Z., Li, X., Han, M., and Wu, Z.** (2015). Genome-wide analysis and functional  
1282 identification of the annexin gene family in maize (*Zea mays* L.). Plant Omics **8**,  
1283 420-428.

1284 **Zhao, P., and Sun, M.X.** (2015). The maternal-to-zygotic transition in higher plants:  
1285 Available approaches, critical limitations, and technical requirements. Curr Top  
1286 Dev Biol **113**, 373-398.

1287 **Zhao, P., Begcy, K., Dresselhaus, T., and Sun, M.X.** (2017). Does early  
1288 embryogenesis in eudicots and monocots involve the same mechanism and  
1289 molecular players? Plant Physiol **173**, 130-142.

1290 **Zheng, B., He, H., Zheng, Y., Wu, W., and McCormick, S.** (2014). An ARID  
1291 domain-containing protein within nuclear bodies is required for sperm cell  
1292 formation in *Arabidopsis thaliana*. PLoS Genet **10**, e1004421.

1293 **Zhou, D.X., Bisanz-Seyer, C., and MacHe, R.** (1995). Molecular cloning of a small  
1294 DNA binding protein with specificity for a tissue-specific negative element within  
1295 the rps1 promoter. Nucl Acids Res **23**, 1165-1169.

1296

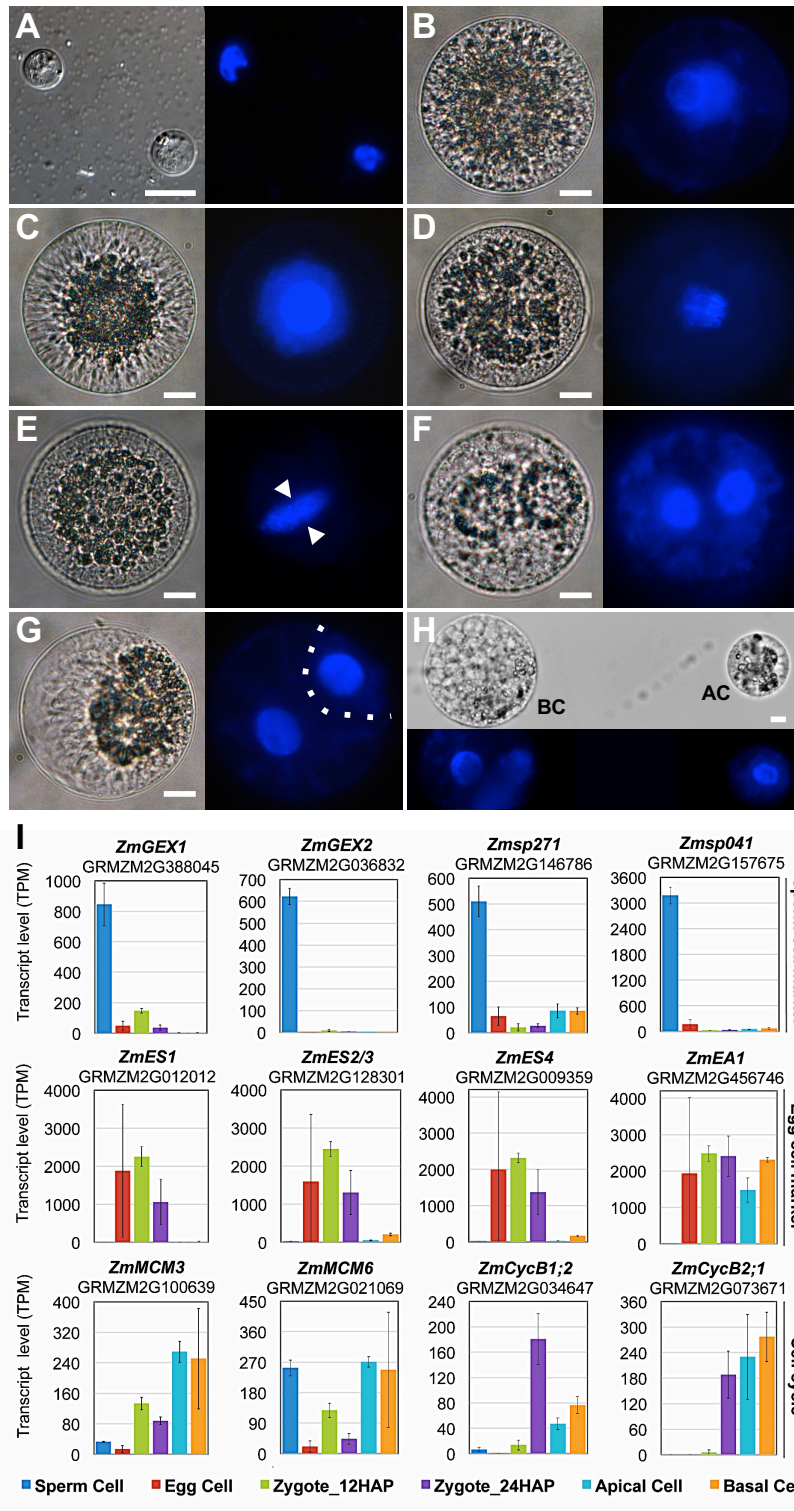


**Figure 1. Time course of zygote development and validation of RNA-Seq data.** (A) Sperm cells. (B) Egg cell. (C) Zygote at 24 hours after pollination (HAP). (D) Zygote at 30 HAP at anaphase. (E) Zygote at 35 HAP at telophase. Arrowheads indicate phragmoplast between daughter chromosome sets. (F) Zygote at 43 HAP during asymmetric cell division (ACD). (G) Zygote at 48 HAP. Cytokinesis is completed. Dotted line indicates the cell division plane. (H) Apical (AC) and basal cell (BC) have been separated at 54 HAP. Bright field microscopy images are shown on the left and UV images of DAPI stained cells on the right. Scale bars: 10  $\mu$ m. (I) Validation of RNA-Seq data with known genes, as indicated. Top row: Genes preferentially expressed in sperm cells; middle row: Genes highly expressed in egg cells and downregulated after fertilization; bottom row: Expression of cell cycle regulators. Transcript levels are shown as TPM (transcripts per million) values (means  $\pm$  SD) of three biological replicates.

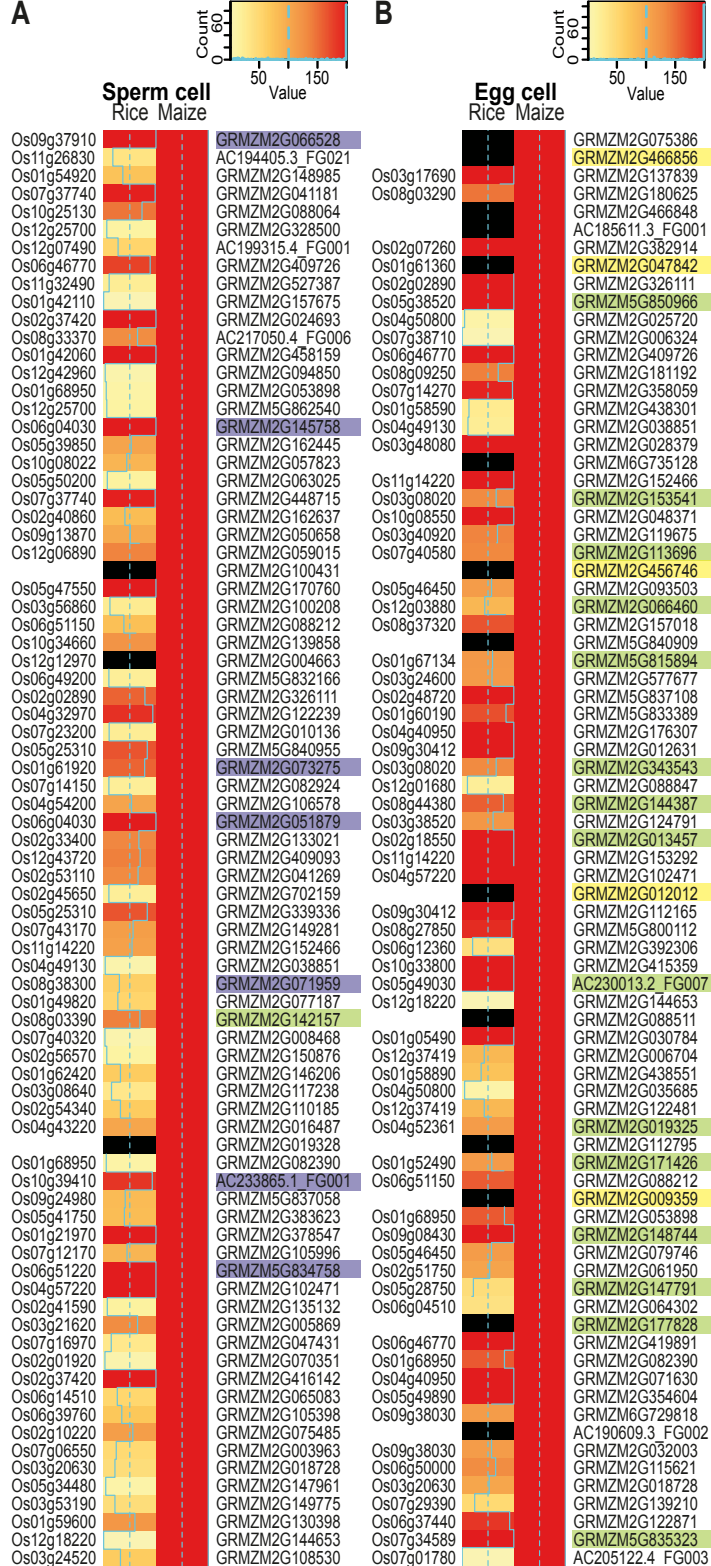


**Figure 2. Heatmap showing a comparison of the 80 most highly expressed genes in maize gametes and their predicted orthologs in the corresponding rice gametes. (A) TOP80 most highly expressed genes in maize sperm cells and (B) TOP80 genes in maize egg cells. Note that all maize genes display a TPM>200 and are thus indicated by red bars. For better visualization, rice and maize gene expression values (TPM) were square root transformed and classified into 80 expression categories using the 0.99th percentile of the data to summarize all higher expression values. Plastid genomes were excluded, as they showed overshooting of expression in the rice data. Non-expressed genes in the rice data and genes lacking a clear homolog are marked by black bars. Orthologous gene information is based on the EnsemblPlants Compara database, The Rice Genome Annotation Project (RGAP), and orthologs from RGAP based on OrthoMCL. Maize genes encoding histones and high-mobility group genes are shaded in purple, proteins involved in translation are in green, and EA1-box proteins and predicted secreted CRPs are in yellow. Proteins were classified according to InterPro.**

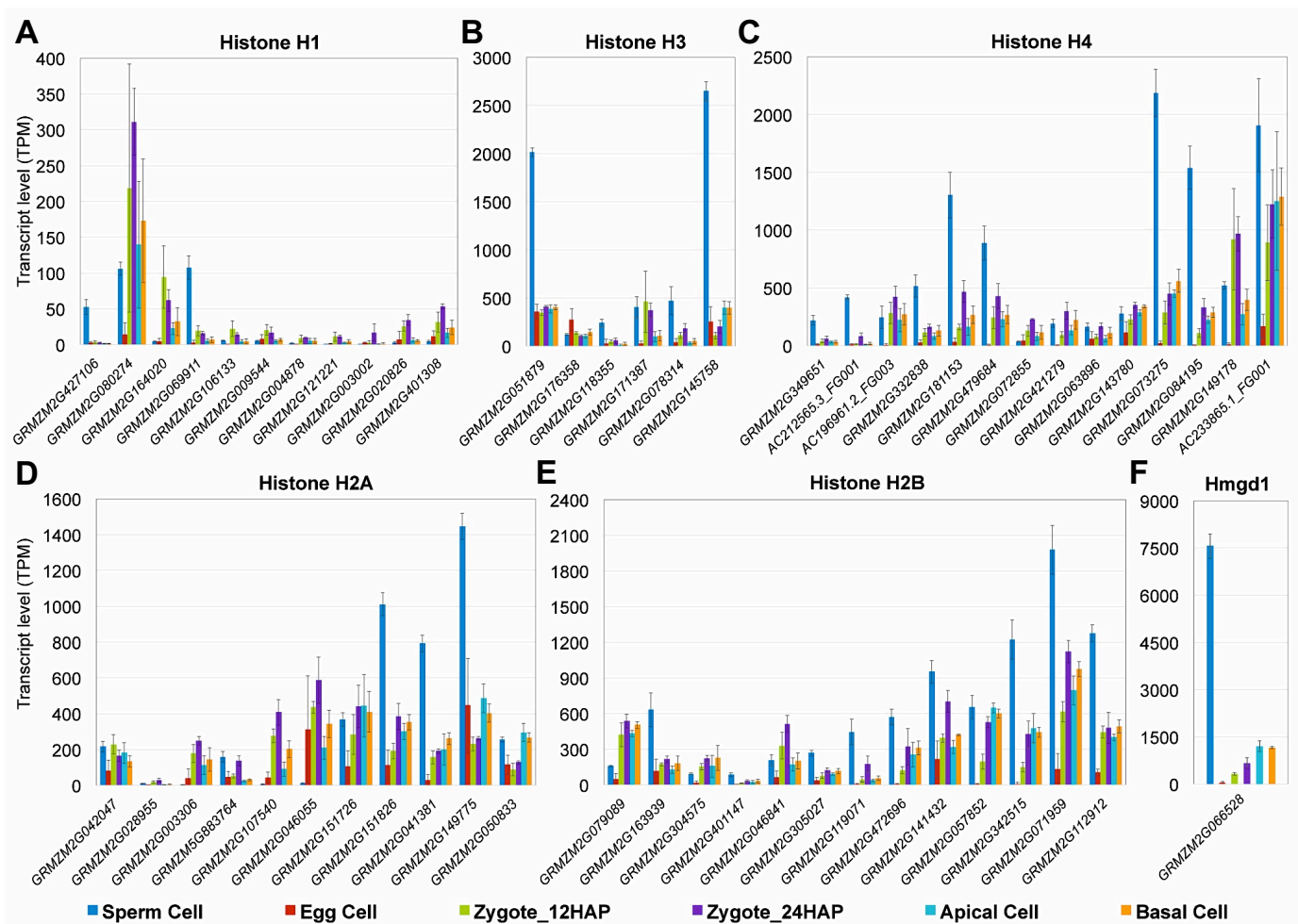


**Figure 3. Expression of major chromatin structure protein genes in maize gametes, zygotes, and daughter cells.** (A) Histone H1, (B) histone H3, (C) histone H4, (D) histone H2A, (E) histone H2B, and (F) high mobility group protein Hmgd1. All significantly expressed genes of the various gene families are presented. See Supplemental Figure S3 for phylogenetic analysis of male-specific and active chromatin-specific variants of histones H3 and H2A. Gene identifiers are listed in Supplemental Table S8 (important gene families). Transcript levels in the cells indicated are given as TPM values (means  $\pm$  SD).

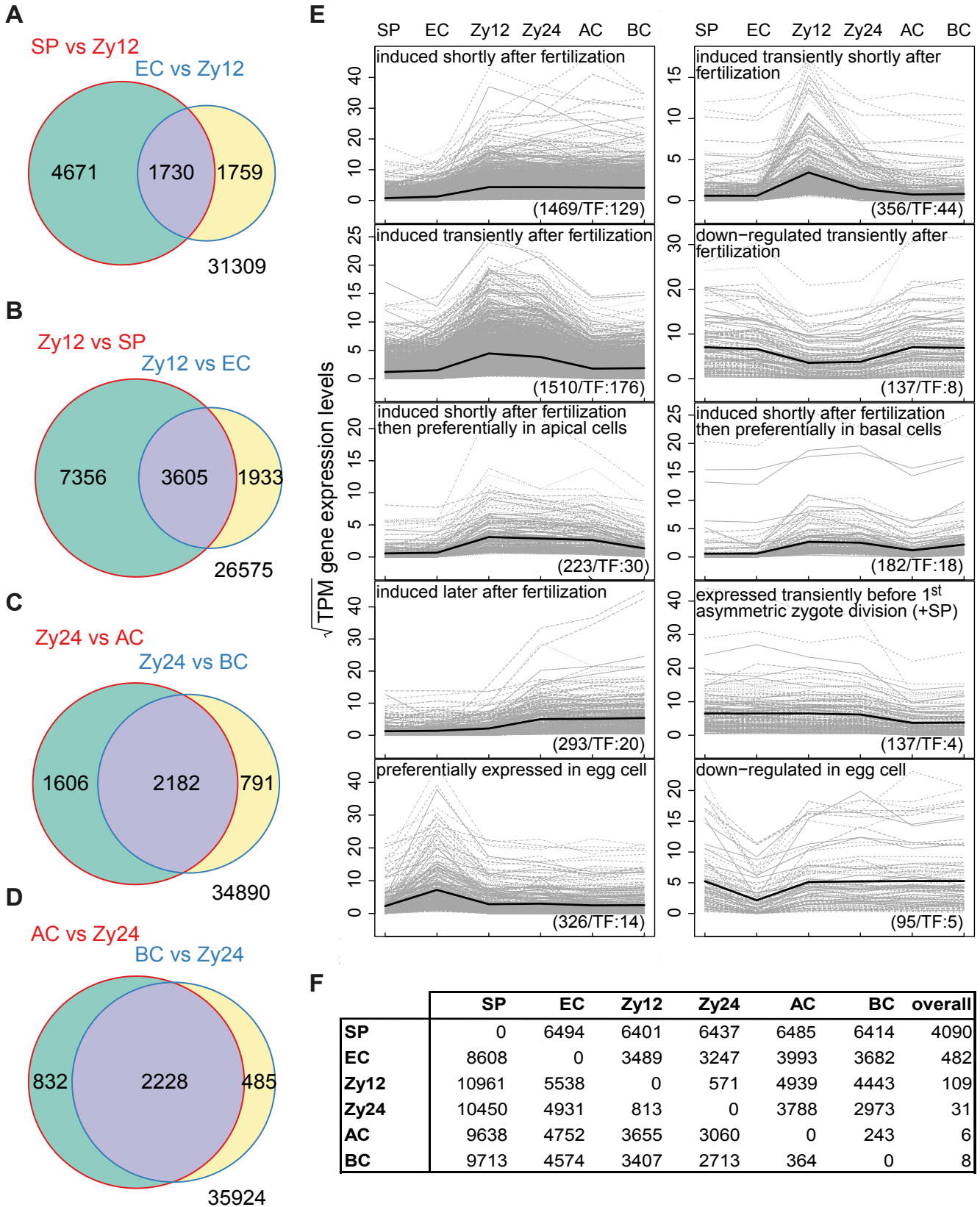


**Figure 4. Gene expression dynamics in maize gametes, zygotes, and two-celled pro-embryo cells.** Genes with a  $abs(\log_2FC) > 1$  and  $p$ -adjusted  $< 0.05$  were considered to be biologically meaningful. **(A)** Comparison of the number of genes induced in sperm cells (SP) and egg cells (EC) versus zygotes at 12 HAP (Zy12). **(B)** Comparisons of genes upregulated in zygotes at 12 HAP versus sperm and egg cells. **(C)** Number of genes induced in zygotes at 24 HAP compared to apical (AC) and basal (BC) cells. **(D)** Comparison of genes upregulated in apical and basal cells versus zygotes at 24 HAP (Zy24). **(E)** Selected gene expression profiles across the specific cell types analyzed (see Supplemental Table S6). The Pearson correlation ( $> 0.9$ ) of square root transformed TPM values per gene and binary profile vectors were used to identify genes belonging to a specific profile. The total number of genes including TFs contained in each profile is shown at the bottom. The mean expression level of all genes per specific cell type is plotted in each profile (black line). **(F)** Table of differentially upregulated genes ( $\log_2FC > 1$ ,  $p$ -adjusted  $< 0.05$ ) of row cell type versus column cell type. The last column show the number of differentially upregulated genes in a row cell type versus all other cell types.

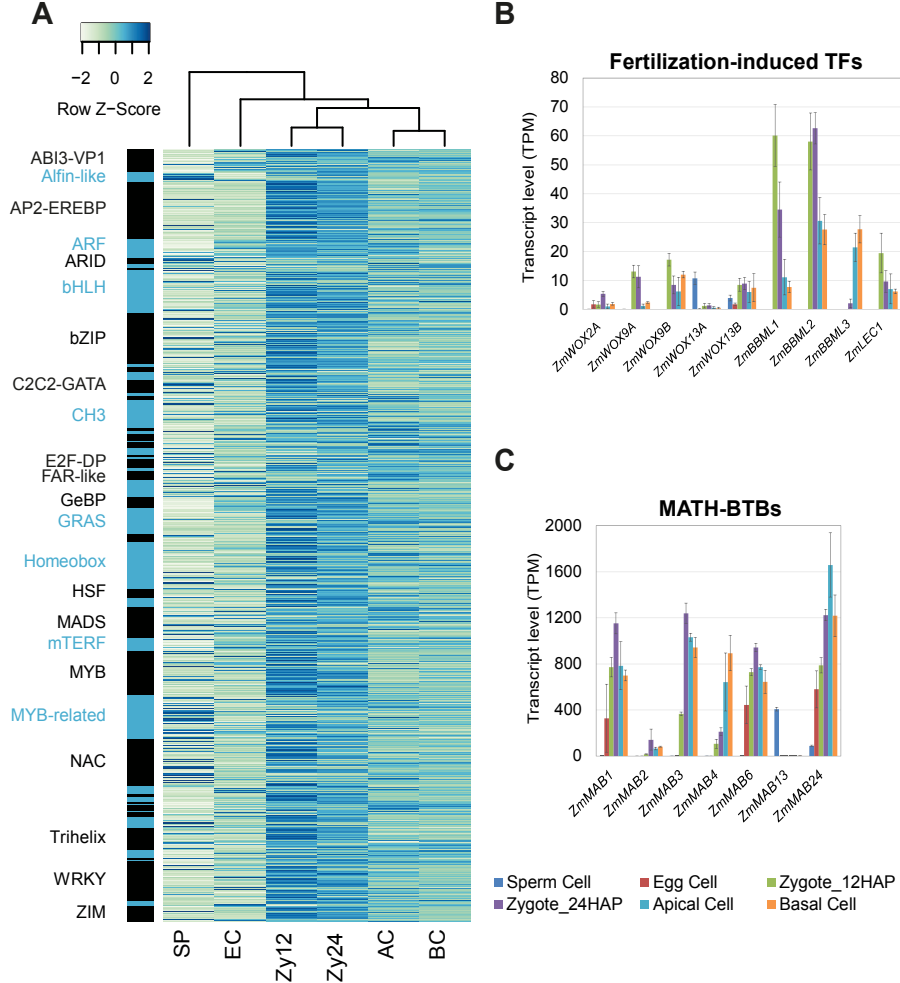


**Figure 5. Expression levels of transcription factor (TF) and MAB genes in gametes, zygotes, and early two-celled pro-embryo cells in maize.** (A) Expression levels of TF genes in gametes and at early developmental stages after fertilization. Genes with  $\text{abs}(\log_2\text{FC}) > 1$  and  $p\text{-adjusted} < 0.05$  in at least one cell type comparison were considered. To make the expression levels comparable across multiple cell types, z-scores were calculated from the square root transformed TPM values corresponding to the number of standard deviations between the cell type-specific expression value and the mean expression value of the respective gene. Genes were ordered by TF classes (black/blue bars). Black and blue fonts were used alternatively to distinguish the various classes. See Supplemental Tables S7 and S8 for details. (B) Expression analysis of selected maize genes encoding homologs of Arabidopsis early embryogenesis-related TFs as well as (C) MATH-BTB (MAB) family genes involved in ACD.

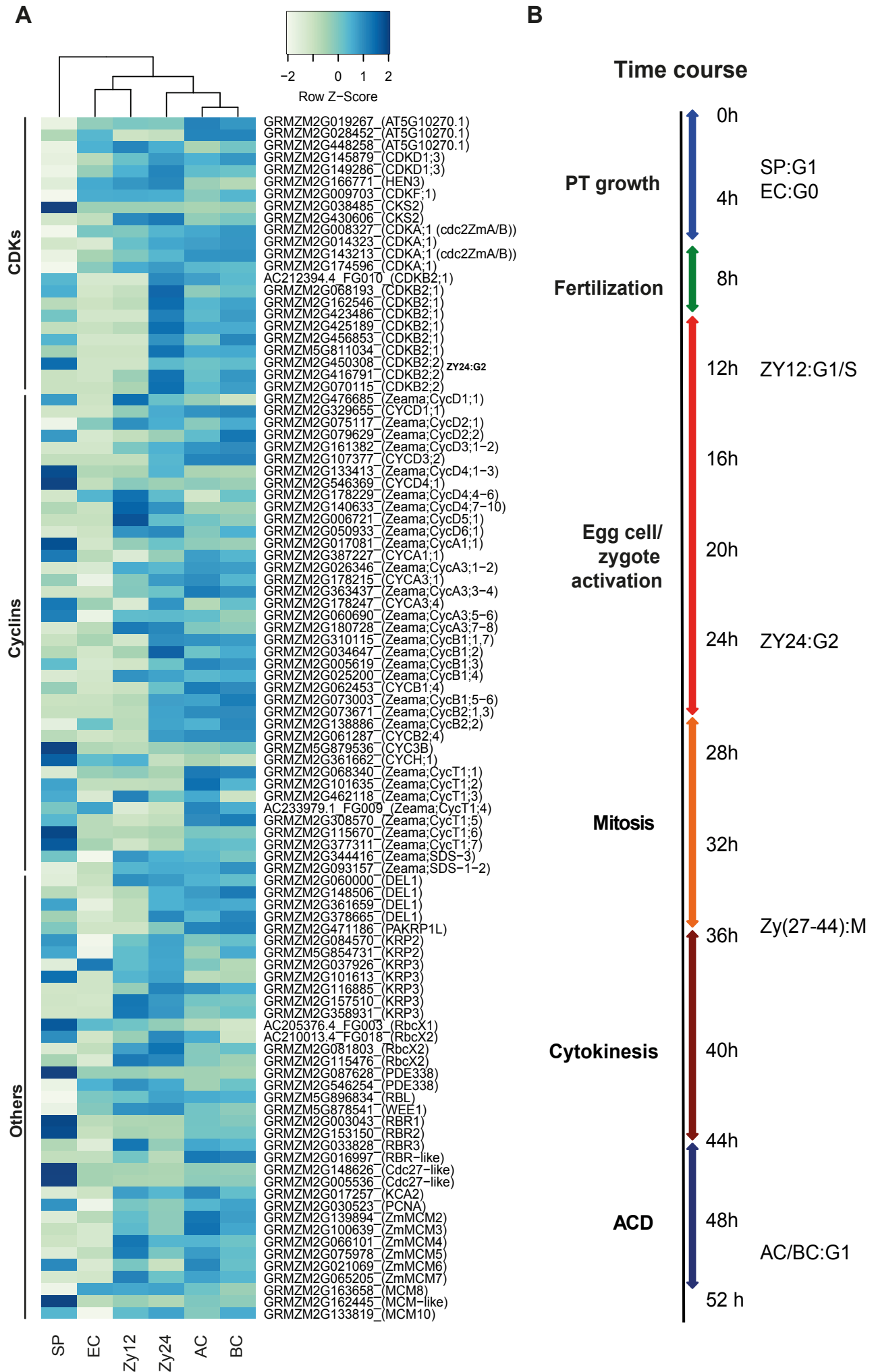


**Figure 6. Gene expression analysis of cell cycle regulators. (A)** Major regulators of the maize cell cycle (Supplemental Table S7). Transformation of gene expression values as described above. Genes were ordered into protein classes based on data from the literature (see Methods for details). **(B)** Summary of the time course of pollen tube (PT) growth, fertilization, and zygote development. Cell cycle stages of the selected cells are indicated based on the currently reported expression data.

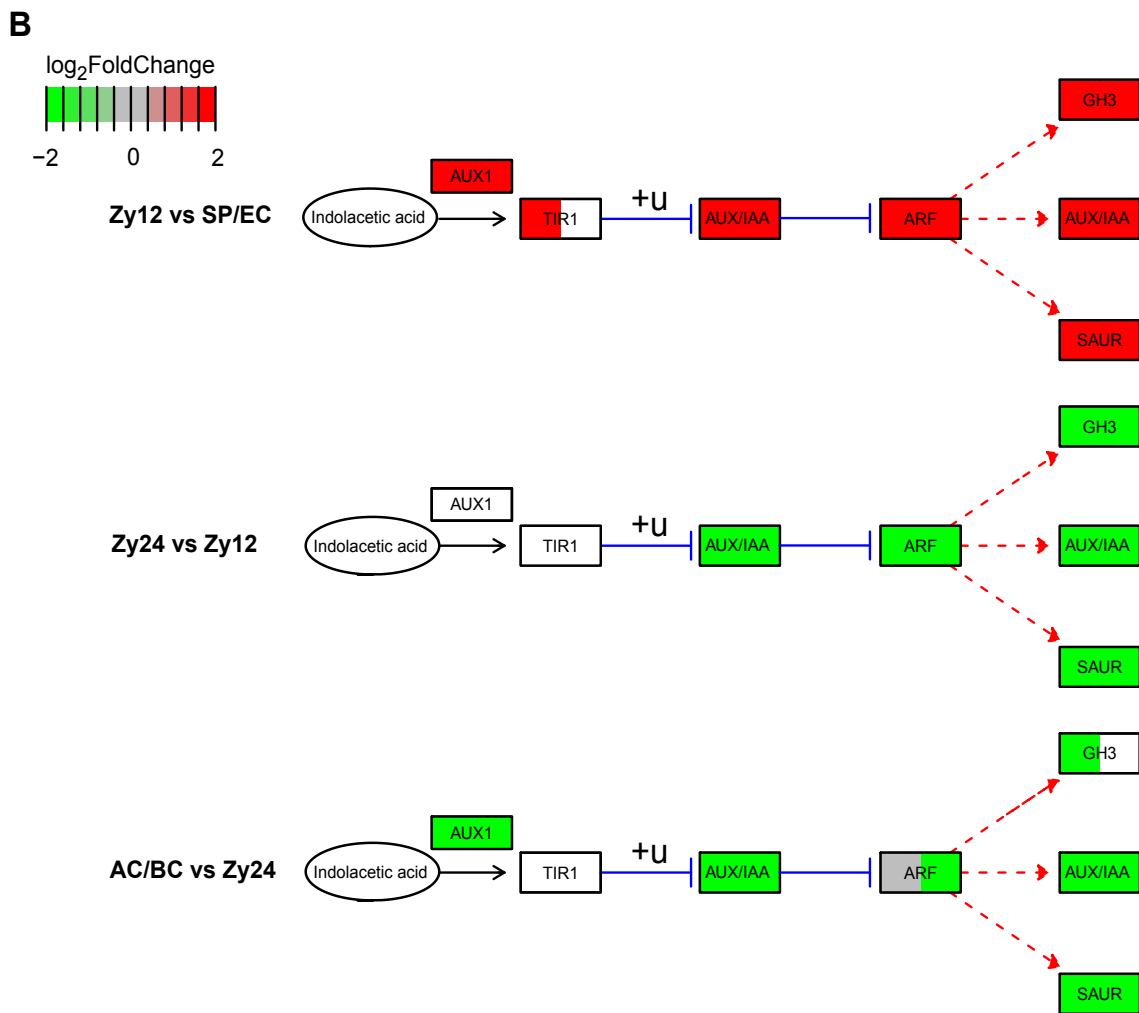
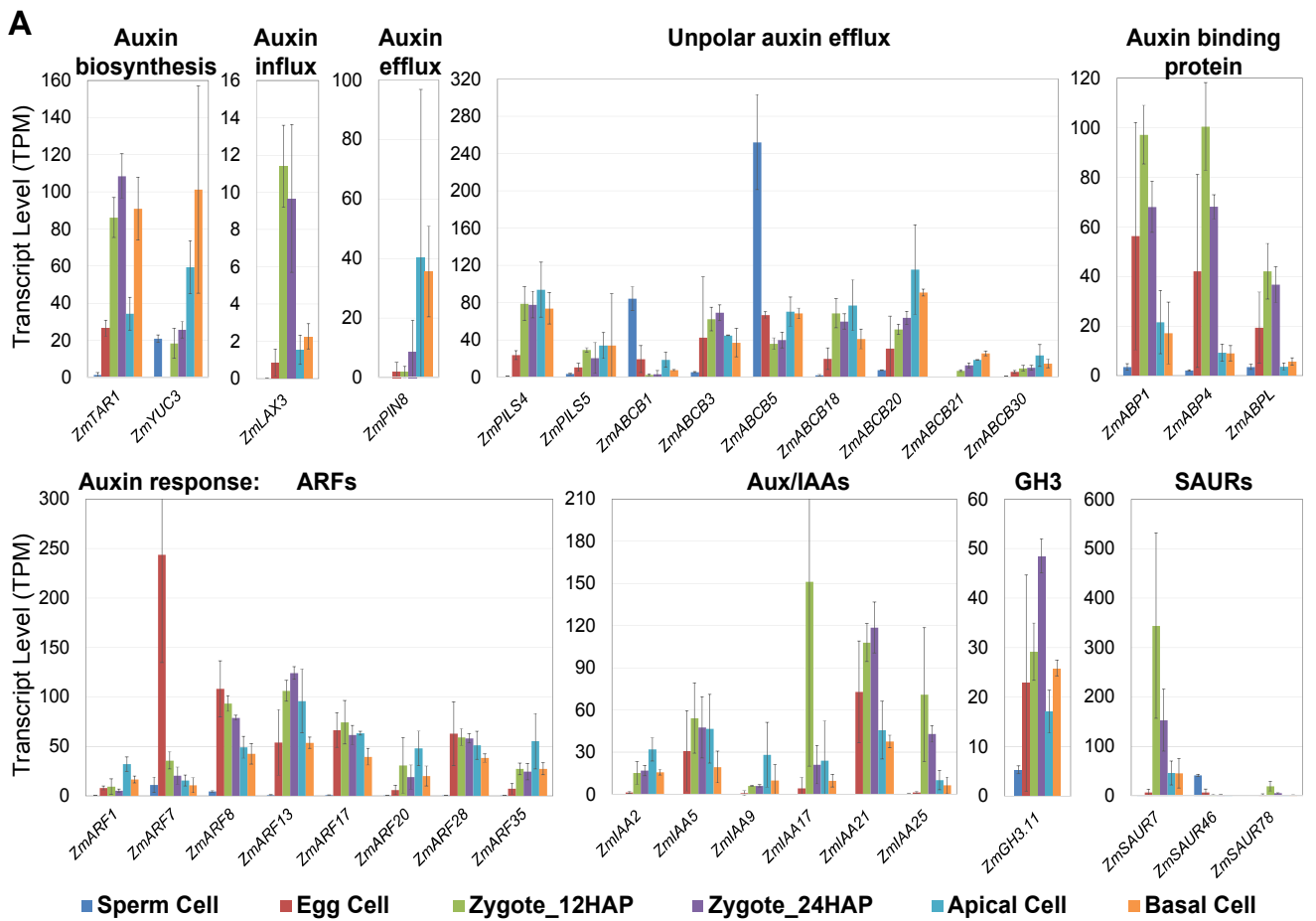


**Figure 7. Analysis of the auxin pathway in gametes, zygotes, and during early embryogenesis. (A)** Expression analysis of the most highly expressed auxin biosynthesis, transport, and auxin response-related genes. **(B)** Auxin pathway analysis using three developmental transitions during zygote development. The median values over the  $\log_2\text{FoldChange}$ s of all differentially expressed genes ( $p$ -adjusted  $< 0.05$ ) from the respective comparison are color-coded in green (downregulated) and red (upregulated). All  $\log_2\text{FoldChange}$ s above 2 or below  $-2$  were set to  $2/-2$  to improve visualization. White boxes: no significant  $\log_2\text{FC}$  found, +u: ubiquitination, blue line: inhibition, dotted gray line: dissociation, red dashed line: expression. Gene pathway based on KEGG analysis. See Supplementary Table 7 for genes.

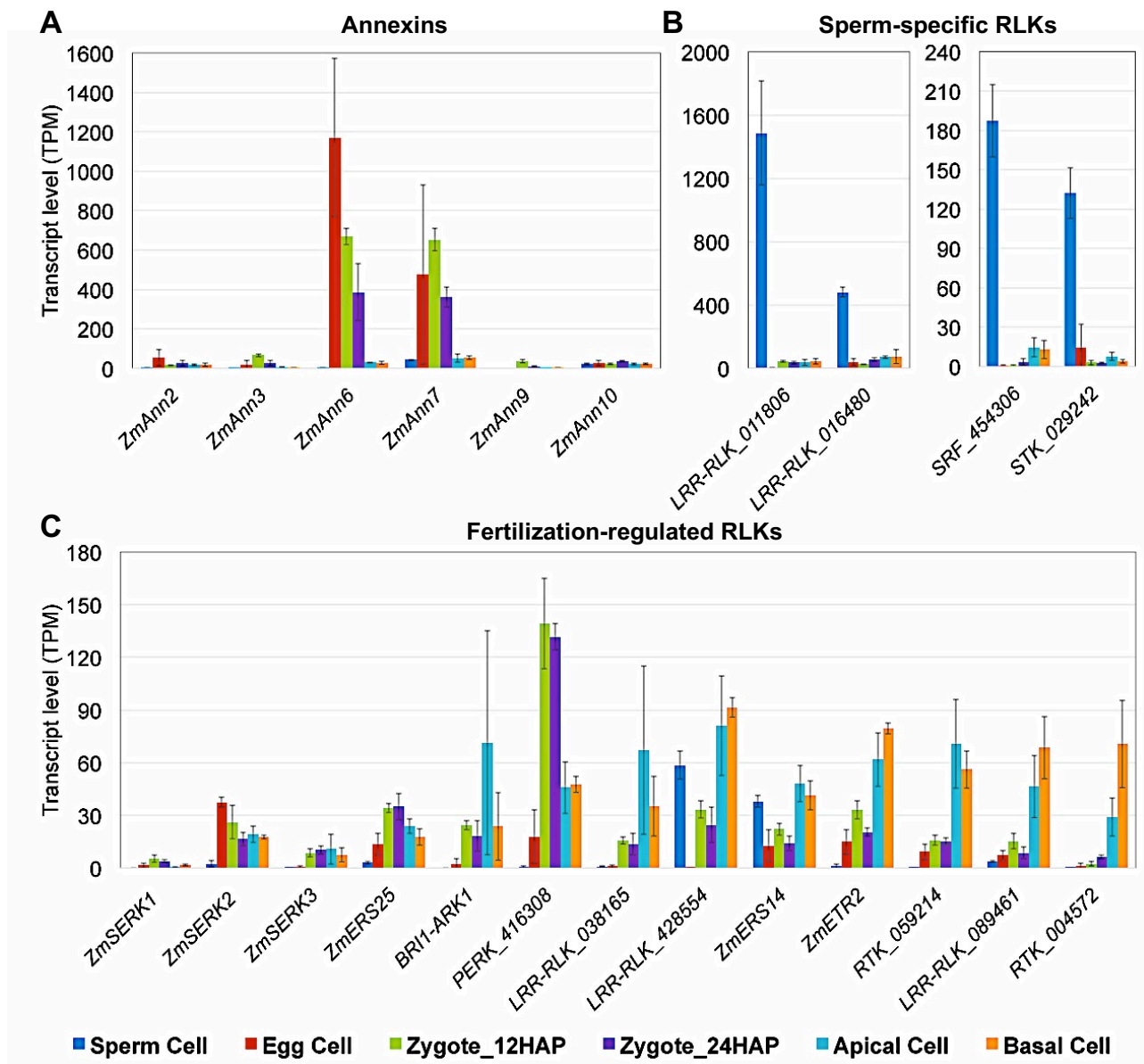


**Figure 8. Expression analysis of selected maize genes with putative roles in signaling during gamete interaction and early embryogenesis.** (A)  $\text{Ca}^{2+}$ -dependent phospholipid-binding annexin family proteins, (B) sperm-specific receptor-like kinases, and (C) fertilization-regulated receptor-like kinases. Gene identifiers are listed in Supplemental Table S7 (important gene families). Transcript levels in the cells indicated are given as TPM values (means  $\pm$  SD).

## Parsed Citations

- Ahmad, K., and Henikoff, S. (2002).** The histone variant H3.3 marks active chromatin by replication-independent nucleosome assembly. *Mol Cell* 9, 1191-1200.  
Pubmed: [Author and Title](#)  
CrossRef: [Author and Title](#)  
Google Scholar: [Author Only](#) [Title Only](#) [Author and Title](#)
- Am, B., Lohse, M., and Usadel, B. (2014).** Trimmomatic: a flexible trimmer for Illumina sequence data. *Bioinformatics* 30, 2114-2120.  
Pubmed: [Author and Title](#)  
CrossRef: [Author and Title](#)  
Google Scholar: [Author Only](#) [Title Only](#) [Author and Title](#)
- Amien, S., Kliwer, I., Marton, M.L., Debener, T., Geiger, D., Becker, D., and Dresselhaus, T. (2010).** Defensin-like ZmES4 mediates pollen tube burst in maize via opening of the potassium channel KZM1. *PLoS Biol* 8, e1000388.  
Pubmed: [Author and Title](#)  
CrossRef: [Author and Title](#)  
Google Scholar: [Author Only](#) [Title Only](#) [Author and Title](#)
- Anderson, S.N., Johnson, C.S., Jones, D.S., Conrad, L.J., Gou, X., Russell, S.D., and Sundaresan, V. (2013).** Transcriptomes of isolated *Oryza sativa* gametes characterized by deep sequencing: evidence for distinct sex-dependent chromatin and epigenetic states before fertilization. *Plant J* 76, 729-741.  
Pubmed: [Author and Title](#)  
CrossRef: [Author and Title](#)  
Google Scholar: [Author Only](#) [Title Only](#) [Author and Title](#)
- Autran, D., Baroux, C., Raissig, M.T., Lenormand, T., Wittig, M., Grob, S., Steimer, A., Barann, M., Klostermeier, U.C., Leblanc, O., Vielle-Calzada, J.P., Rosenstiel, P., Grimanelli, D., Grossniklaus, U. (2011).** Maternal epigenetic pathways control parental contributions to *Arabidopsis* early embryogenesis. *Cell* 145, 707-719.  
Pubmed: [Author and Title](#)  
CrossRef: [Author and Title](#)  
Google Scholar: [Author Only](#) [Title Only](#) [Author and Title](#)
- Baroux, C., and Grossniklaus, U. (2015).** The maternal-to-zygotic transition in flowering plants: Evidence, mechanisms, and plasticity. *Curr Top Dev Biol* 113, 351-371.  
Pubmed: [Author and Title](#)  
CrossRef: [Author and Title](#)  
Google Scholar: [Author Only](#) [Title Only](#) [Author and Title](#)
- Benjamini, Y., and Hochberg, Y. (1995).** Controlling the false discovery rate: a practical and powerful approach to multiple testing. *J Royal Statist Soc Ser B* 57, 289-300.  
Pubmed: [Author and Title](#)  
CrossRef: [Author and Title](#)  
Google Scholar: [Author Only](#) [Title Only](#) [Author and Title](#)
- Borges, F., Gomes, G., Gardner, R., Moreno, N., McCormick, S., Feijo, J.A., and Becker, J.D. (2008).** Comparative transcriptomics of *Arabidopsis* sperm cells. *Plant Physiol* 148, 1168-1181.  
Pubmed: [Author and Title](#)  
CrossRef: [Author and Title](#)  
Google Scholar: [Author Only](#) [Title Only](#) [Author and Title](#)
- Boutillier, K., Offringa, R., Sharma, V.K., Kieft, H., Ouellet, T., Zhang, L., Hattori, J., Liu, C.-M., van Lammeren, A.A.M., Miki, B.L.A., Custers, J.B.M., and van Lookeren Campagne, M.M. (2002).** Ectopic expression of BABY BOOM triggers a conversion from vegetative to embryonic growth. *Plant Cell* 14, 1737-1749.  
Pubmed: [Author and Title](#)  
CrossRef: [Author and Title](#)  
Google Scholar: [Author Only](#) [Title Only](#) [Author and Title](#)
- Breuninger, H., Rikirsch, E., Hermann, M., Ueda, M., and Laux, T. (2008).** Differential expression of WOX genes mediates apical-basal axis formation in the *Arabidopsis* embryo. *Dev Cell* 14, 867-876.  
Pubmed: [Author and Title](#)  
CrossRef: [Author and Title](#)  
Google Scholar: [Author Only](#) [Title Only](#) [Author and Title](#)
- Budkevich, T.V., Timchenko, A.A., Tiktopulo, E.I., Negrutskii, B.S., Shalak, V.F., Petrushenko, Z.M., Aksenov, V.L., Willumeit, R., Kohlbrecher, J., Serdyuk, I.N., and El'skaya, A.V. (2002).** Extended conformation of mammalian translation elongation factor 1A in solution. *Biochemistry* 41, 15342-15349.  
Pubmed: [Author and Title](#)  
CrossRef: [Author and Title](#)  
Google Scholar: [Author Only](#) [Title Only](#) [Author and Title](#)
- Buendía-Monreal, M., Rentería-Canett, I., Guerrero-Andrade, O., Bravo-Alberto, C.E., Martínez-Castilla, L.P., García, E., and Vázquez-Ramos, J.M. (2011).** The family of maize D-type cyclins: genomic organization, phylogeny and expression patterns. *Physiol Plantarum* 143, 297-308.

Pubmed: [Author and Title](#)  
CrossRef: [Author and Title](#)  
Google Scholar: [Author Only Title Only Author and Title](#)

**Chen, J., Lausser, A., and Dresselhaus, T. (2014). Hormonal responses during early embryogenesis in maize. *Biochem Soc Transact* 42, 325-331.**

Pubmed: [Author and Title](#)  
CrossRef: [Author and Title](#)  
Google Scholar: [Author Only Title Only Author and Title](#)

**Chen, J., Gutjahr, C., Bleckmann, A., and Dresselhaus, T. (2015). Calcium signaling during reproduction and biotrophic fungal interactions in plants. *Mol Plant* 8, 595-611.**

Pubmed: [Author and Title](#)  
CrossRef: [Author and Title](#)  
Google Scholar: [Author Only Title Only Author and Title](#)

**Chettoor, A.M., Givan, S.A., Cole, R.A., Coker, C.T., Unger-Wallace, E., Vejlupkova, Z., Vollbrecht, E., Fowler, J.E., Evans, M.M. (2014). Discovery of novel transcripts and gametophytic functions via RNA-seq analysis of maize gametophytic transcriptomes. *Genome Biol* 15, 414.**

Pubmed: [Author and Title](#)  
CrossRef: [Author and Title](#)  
Google Scholar: [Author Only Title Only Author and Title](#)

**Chevalier, F., Perazza, D., Laporte, F., Le Héanff, G., Hornitschek, P., Bonneville, J.-M., Herzog, M., and Vachon, G. (2008). GeBP and GeBP-like proteins are noncanonical leucine-zipper transcription factors that regulate cytokinin response in *Arabidopsis*. *Plant Physiol* 146, 1142-1154.**

Pubmed: [Author and Title](#)  
CrossRef: [Author and Title](#)  
Google Scholar: [Author Only Title Only Author and Title](#)

**Cordts, S., Bantin, J., Wittich, P.E., Kranz, E., Lörz, H., and Dresselhaus, T. (2001). ZmES genes encode peptides with structural homology to defensins and are specifically expressed in the female gametophyte of maize. *Plant J* 25, 103-114.**

Pubmed: [Author and Title](#)  
CrossRef: [Author and Title](#)  
Google Scholar: [Author Only Title Only Author and Title](#)

**Cui, Y., Dinman, J.D., Kinzy, T.G., and Peltz, S.W. (1998). The Mof2/Sui1 protein is a general monitor of translational accuracy. *Mol Cell Biol* 18, 1506-1516.**

Pubmed: [Author and Title](#)  
CrossRef: [Author and Title](#)  
Google Scholar: [Author Only Title Only Author and Title](#)

**Dante, R.A., Larkins, B.A., and Sabelli, P.A. (2014). Cell cycle control and seed development. *Front Plant Sci* 5, 493.**

Pubmed: [Author and Title](#)  
CrossRef: [Author and Title](#)  
Google Scholar: [Author Only Title Only Author and Title](#)

**Deal, R.B., and Henikoff, S. (2011). Histone variants and modifications in plant gene regulation. *Curr Opin Plant Biol* 14, 116-122.**

Pubmed: [Author and Title](#)  
CrossRef: [Author and Title](#)  
Google Scholar: [Author Only Title Only Author and Title](#)

**Del Toro-De León, G., García-Aguilar, M., and Gillmor, C.S. (2014). Non-equivalent contributions of maternal and paternal genomes to early plant embryogenesis. *Nature* 514, 624-627.**

Pubmed: [Author and Title](#)  
CrossRef: [Author and Title](#)  
Google Scholar: [Author Only Title Only Author and Title](#)

**Dobin, A., Davis, C.A., Schlesinger, F., Drenkow, J., Zaleski, C., Jha, S., Batut, P., Chaisson, M., and Gingeras, T.R. (2013). STAR: Ultrafast universal RNA-Seq aligner. *Bioinformatics* 29, 15-21.**

Pubmed: [Author and Title](#)  
CrossRef: [Author and Title](#)  
Google Scholar: [Author Only Title Only Author and Title](#)

**Dresselhaus, T., Cordts, S., and Lörz, H. (1999a). A transcript encoding translation initiation factor eIF-5A is stored in unfertilized egg cells of maize. *Plant Mol Biol* 39, 1063-1071.**

Pubmed: [Author and Title](#)  
CrossRef: [Author and Title](#)  
Google Scholar: [Author Only Title Only Author and Title](#)

**Dresselhaus, T., Lausser, A., and Márton, M.L. (2011). Using maize as a model to study pollen tube growth and guidance, cross-incompatibility and sperm delivery in grasses. *Annals Bot* 108, 727-737.**

Pubmed: [Author and Title](#)  
CrossRef: [Author and Title](#)  
Google Scholar: [Author Only Title Only Author and Title](#)

Dresselhaus, T., Sprunck, S., and Wessel, G.M. (2016). Fertilization mechanisms in flowering plants. *Curr Biol* 26, R125-139.

Pubmed: [Author and Title](#)

CrossRef: [Author and Title](#)

Google Scholar: [Author Only](#) [Title Only](#) [Author and Title](#)

Dresselhaus, T., Srilunchang, K.-O., Leljak-Levanic, D., Schreiber, D.N., and Garg, P. (2006). The fertilization-induced DNA replication factor MCM6 of maize shuttles between cytoplasm and nucleus, and is essential for plant growth and development. *Plant Physiol* 140, 512-527.

Pubmed: [Author and Title](#)

CrossRef: [Author and Title](#)

Google Scholar: [Author Only](#) [Title Only](#) [Author and Title](#)

Dresselhaus, T., Cordts, S., Heuer, S., Sauter, M., Lörz, H., and Kranz, E. (1999b). Novel ribosomal genes from maize are differentially expressed in the zygotic and somatic cell cycles. *Mol Gen Genet* 261, 416-427.

Pubmed: [Author and Title](#)

CrossRef: [Author and Title](#)

Google Scholar: [Author Only](#) [Title Only](#) [Author and Title](#)

Dupuis, I., Roeckel, P., Matthys-Rochon, E., and Dumas, C. (1987). Procedure to isolate viable sperm cells from corn (*Zea mays* L.) pollen grains. *Plant Physiol* 85, 876-878.

Pubmed: [Author and Title](#)

CrossRef: [Author and Title](#)

Google Scholar: [Author Only](#) [Title Only](#) [Author and Title](#)

Engel, M.L., Chaboud, A., Dumas, C., and McCormick, S. (2003). Sperm cells of *Zea mays* have a complex complement of mRNAs. *Plant J* 34, 697-707.

Pubmed: [Author and Title](#)

CrossRef: [Author and Title](#)

Google Scholar: [Author Only](#) [Title Only](#) [Author and Title](#)

Friml, J., Vieten, A., Sauer, M., Weijers, D., Schwarz, H., Hamann, T., Offringa, R., and Jurgens, G. (2003). Efflux-dependent auxin gradients establish the apical-basal axis of *Arabidopsis*. *Nature* 426, 147-153.

Pubmed: [Author and Title](#)

CrossRef: [Author and Title](#)

Google Scholar: [Author Only](#) [Title Only](#) [Author and Title](#)

Gerke, V., Creutz, C.E., and Moss, S.E. (2005). Annexins: linking Ca<sup>2+</sup> signalling to membrane dynamics. *Nat Rev Mol Cell Biol* 6, 449-461.

Pubmed: [Author and Title](#)

CrossRef: [Author and Title](#)

Google Scholar: [Author Only](#) [Title Only](#) [Author and Title](#)

Grimanelli, D., Perotti, E., Ramirez, J., and Leblanc, O. (2005) Timing of the maternal-to-zygotic transition during early seed development in maize. *Plant Cell* 17, 1061-1072.

Pubmed: [Author and Title](#)

CrossRef: [Author and Title](#)

Google Scholar: [Author Only](#) [Title Only](#) [Author and Title](#)

Guo, S., and Kempfues, K.J. (1995). par-1, a gene required for establishing polarity in *C. elegans* embryos, encodes a putative Ser/Thr kinase that is asymmetrically distributed. *Cell* 81, 611-620.

Pubmed: [Author and Title](#)

CrossRef: [Author and Title](#)

Google Scholar: [Author Only](#) [Title Only](#) [Author and Title](#)

Hecht, V., Vielle-Calzada, J.-P., Hartog, M.V., Schmidt, E.D.L., Boutilier, K., Grossniklaus, U., and de Vries, S.C. (2001). The *Arabidopsis* somatic embryogenesis receptor kinase 1 gene is expressed in developing ovules and embryos and enhances embryogenic competence in culture. *Plant Physiol* 127, 803-816.

Pubmed: [Author and Title](#)

CrossRef: [Author and Title](#)

Google Scholar: [Author Only](#) [Title Only](#) [Author and Title](#)

Hu, X., Cheng, X., Jiang, H., Zhu, S., Cheng, B., and Xiang, Y. (2010). Genome-wide analysis of cyclins in maize (*Zea mays*). *Genet Mol Res* 9, 1490-1503.

Pubmed: [Author and Title](#)

CrossRef: [Author and Title](#)

Google Scholar: [Author Only](#) [Title Only](#) [Author and Title](#)

Ingouff, M., Rademacher, S., Holec, S., Šoljic, L., Xin, N., Readshaw, A, Foo, S.H., Lahouze, B., Sprunck, S., and Berger, F. (2010). Zygotic resetting of the HISTONE 3 variant repertoire participates in epigenetic reprogramming in *Arabidopsis*. *Curr Biol* 20, 2137-2143.

Pubmed: [Author and Title](#)

CrossRef: [Author and Title](#)

Google Scholar: [Author Only](#) [Title Only](#) [Author and Title](#)

Juranic, M., Srilunchang, K.-o., Krohn, N.G., Leljak-Levanic, D., Sprunck, S., and Dresselhaus, T. (2012). Germline-specific MATH-BTB substrate adaptor MAB1 regulates spindle length and nuclei identity in maize. *Plant Cell* 24, 4974-4991.

Pubmed: [Author and Title](#)  
CrossRef: [Author and Title](#)  
Google Scholar: [Author Only Title Only Author and Title](#)

**Kawahara, Y., La Bastide, M., Hamilton, J.P., Kanamori, H., McCombie, W.R., Ouyang, S., Schwartz, D.C., Tanaka, T., Wu, J., Zhou, S., Childs, K.L., Davidson, R.M., Lin, H., Quesada-Ocampo, L., Vaillancourt, B., Sakai, H., Lee, S.S., Kim, J., Numa, H., Itoh, T., Buell, C.R., and Matsumoto, T. (2013). Improvement of the *Oryza sativa* Nipponbare reference genome using next generation sequence and optical map data. *Rice* 6, 4.**

Pubmed: [Author and Title](#)  
CrossRef: [Author and Title](#)  
Google Scholar: [Author Only Title Only Author and Title](#)

**Kim, D., Pertea, G., Trapnell, C., Pimentel, H., Kelley, R., and Salzberg, S.L. (2013). TopHat2: accurate alignment of transcriptomes in the presence of insertions, deletions and gene fusions. *Genome Biol* 14, R36.**

Pubmed: [Author and Title](#)  
CrossRef: [Author and Title](#)  
Google Scholar: [Author Only Title Only Author and Title](#)

**Kleine, T. (2012). *Arabidopsis thaliana* mTERF proteins: evolution and functional classification. *Front Plant Sci* 3, 233.**

Pubmed: [Author and Title](#)  
CrossRef: [Author and Title](#)  
Google Scholar: [Author Only Title Only Author and Title](#)

**Kranz, E., Bautor, J., and Lorz, H. (1991). In vitro fertilization of single, isolated gametes of maize mediated by electrofusion. *Sex Plant Reprod* 4, 12-16.**

Pubmed: [Author and Title](#)  
CrossRef: [Author and Title](#)  
Google Scholar: [Author Only Title Only Author and Title](#)

**Lee, M.T., Bonneau, A.R., and Giraldez, A.J. (2014). Zygotic genome activation during the maternal-to-zygotic transition. *Annu Rev Cell Dev Biol* 30, 581-613.**

Pubmed: [Author and Title](#)  
CrossRef: [Author and Title](#)  
Google Scholar: [Author Only Title Only Author and Title](#)

**Lehti-Shiu, M.D., Adamczyk, B.J., and Fernandez, D.E. (2005). Expression of MADS-box genes during the embryonic phase in *Arabidopsis*. *Plant Mol Biol* 58, 89-107.**

Pubmed: [Author and Title](#)  
CrossRef: [Author and Title](#)  
Google Scholar: [Author Only Title Only Author and Title](#)

**Li, L., Stoeckert, C.J., Jr., and Roos, D.S. (2003). OrthoMCL: identification of ortholog groups for eukaryotic genomes. *Genome Res* 13, 2178-2189.**

Pubmed: [Author and Title](#)  
CrossRef: [Author and Title](#)  
Google Scholar: [Author Only Title Only Author and Title](#)

**Liao, Y., Smyth, G.K., and Shi, W. (2014). featureCounts: an efficient general purpose program for assigning sequence reads to genomic features. *Bioinformatics* 30, 923-930.**

Pubmed: [Author and Title](#)  
CrossRef: [Author and Title](#)  
Google Scholar: [Author Only Title Only Author and Title](#)

**Long, R.M., Singer, R.H., Meng, X., Gonzalez, I., Nasmyth, K., and Jansen, R.P. (1997). Mating type switching in yeast controlled by asymmetric localization of ASH1 mRNA. *Science* 277, 383-387.**

Pubmed: [Author and Title](#)  
CrossRef: [Author and Title](#)  
Google Scholar: [Author Only Title Only Author and Title](#)

**Lotan, T., Ohto, M., Yee, K.M., West, M.A., Lo, R., Kwong, R.W., Yamagishi, K., Fischer, R.L., Goldberg, R.B., and Harada, J.J. (1998). *Arabidopsis* LEAFY COTYLEDON1 is sufficient to induce embryo development in vegetative cells. *Cell* 93, 1195-1205.**

Pubmed: [Author and Title](#)  
CrossRef: [Author and Title](#)  
Google Scholar: [Author Only Title Only Author and Title](#)

**Love, M.I., Huber, W., and Anders, S. (2014). Moderated estimation of fold change and dispersion for RNA-seq data with DESeq2. *Genome Biol* 15, 550.**

Pubmed: [Author and Title](#)  
CrossRef: [Author and Title](#)  
Google Scholar: [Author Only Title Only Author and Title](#)

**Lowe, K., Wu, E., Wang, N., Hoerster, G., Hastings, C., Cho, M.J., Scelonge, C., Lenderts, B., Chamberlin, M., Cushatt, J., Wang, L., Ryan, L., Khan, T., Chow-Yiu, J., Hua, W., Yu, M., Banh, J., Bao, Z., Brink, K., Igo, E., Rudrappa, B., Shamseer, P.M., Bruce, W., Newman, L., Shen, B., Zheng, P., Bidney, D., Falco, S.C., Register, I.J., Zhao, Z.Y., Xu, D., Jones, T.J., and Gordon-Kamm, W.J. (2016). Morphogenic regulators Baby Boom and Wuschel improve monocot transformation. *Plant Cell* 28, 1998-2015.**

- Pubmed: [Author and Title](#)  
CrossRef: [Author and Title](#)  
Google Scholar: [Author Only](#) [Title Only](#) [Author and Title](#)
- Maiorano, D., Lutzmann, M., and Mechali, M. (2006).** MCM proteins and DNA replication. *Curr Opin Cell Biol* 18, 130-136.  
Pubmed: [Author and Title](#)  
CrossRef: [Author and Title](#)  
Google Scholar: [Author Only](#) [Title Only](#) [Author and Title](#)
- Martin, M. (2011).** Cutadapt removes adapter sequences from high-throughput sequencing reads. *EMBnet J* 17, 10-12.  
Pubmed: [Author and Title](#)  
CrossRef: [Author and Title](#)  
Google Scholar: [Author Only](#) [Title Only](#) [Author and Title](#)
- Márton, M.L., Cordts, S., Broadhvest, J., and Dresselhaus, T. (2005).** Micropylar pollen tube guidance by egg apparatus 1 of maize. *Science* 307, 573-576.  
Pubmed: [Author and Title](#)  
CrossRef: [Author and Title](#)  
Google Scholar: [Author Only](#) [Title Only](#) [Author and Title](#)
- Meijer, M., and Murray, J.A. (2001).** Cell cycle controls and the development of plant form. *Curr Opin Plant Biol* 4, 44-49.  
Pubmed: [Author and Title](#)  
CrossRef: [Author and Title](#)  
Google Scholar: [Author Only](#) [Title Only](#) [Author and Title](#)
- Mitsuda, N., Isono, T., and Sato, M.H. (2003).** Arabidopsis CAMTA family proteins enhance V-PPase expression in pollen. *Plant Cell Physiol* 44, 975-981.  
Pubmed: [Author and Title](#)  
CrossRef: [Author and Title](#)  
Google Scholar: [Author Only](#) [Title Only](#) [Author and Title](#)
- Nodine, M.D., and Bartel, D.P. (2012).** Maternal and paternal genomes contribute equally to the transcriptome of early plant embryos. *Nature* 482, 94-97.  
Pubmed: [Author and Title](#)  
CrossRef: [Author and Title](#)  
Google Scholar: [Author Only](#) [Title Only](#) [Author and Title](#)
- Okada, T., Endo, M., Singh, M.B., and Bhalla, P.L. (2005).** Analysis of the histone H3 gene family in Arabidopsis and identification of the male-gamete-specific variant AtMGH3. *Plant J* 44, 557-568.  
Pubmed: [Author and Title](#)  
CrossRef: [Author and Title](#)  
Google Scholar: [Author Only](#) [Title Only](#) [Author and Title](#)
- Ouyang, S., Zhu, W., Hamilton, J., Lin, H., Campbell, M., Childs, K., Thibaud-Nissen, F., Malek, R.L., Lee, Y., Zheng, L., Orvis, J., Haas, B., Wortman, J., and Buell, C.R. (2007).** The TIGR rice genome annotation resource: improvements and new features. *Nucl Acids Res* 35, D883-887.  
Pubmed: [Author and Title](#)  
CrossRef: [Author and Title](#)  
Google Scholar: [Author Only](#) [Title Only](#) [Author and Title](#)
- Ouyang, X., Li, J., Li, G., Li, B., Chen, B., Shen, H., Huang, X., Mo, X., Wan, X., Lin, R., Li, S., Wang, H., and Deng, X.W. (2011).** Genome-wide binding site analysis of FAR-RED ELONGATED HYPOCOTYL3 reveals its novel function in Arabidopsis development. *Plant Cell* 23, 2514-2535.  
Pubmed: [Author and Title](#)  
CrossRef: [Author and Title](#)  
Google Scholar: [Author Only](#) [Title Only](#) [Author and Title](#)
- Petrášek, J., and Friml, J. (2009).** Auxin transport routes in plant development. *Development* 136, 2675-2688.  
Pubmed: [Author and Title](#)  
CrossRef: [Author and Title](#)  
Google Scholar: [Author Only](#) [Title Only](#) [Author and Title](#)
- Pintard, L., Willis, J.H., Willems, A., Johnson, J.-L.F., Srayko, M., Kurz, T., Glaser, S., Mains, P.E., Tyers, M., Bowerman, B., and Peter, M. (2003).** The BTB protein MEL-26 is a substrate-specific adaptor of the CUL-3 ubiquitin-ligase. *Nature* 425, 311-316.  
Pubmed: [Author and Title](#)  
CrossRef: [Author and Title](#)  
Google Scholar: [Author Only](#) [Title Only](#) [Author and Title](#)
- Ren, H., and Gray, W.M. (2015).** SAUR proteins as effectors of hormonal and environmental signals in plant growth. *Mol Plant* 8, 1153-1164.  
Pubmed: [Author and Title](#)  
CrossRef: [Author and Title](#)  
Google Scholar: [Author Only](#) [Title Only](#) [Author and Title](#)
- Rieseberg, L.H., and Willis, J.H. (2007).** Plant speciation. *Science* 317, 910-914.  
Pubmed: [Author and Title](#)

CrossRef: [Author and Title](#)

Google Scholar: [Author Only Title Only Author and Title](#)

**Russell, S.D., Gou, X., Wong, C.E., Wang, X., Yuan, T., Wei, X., Bhalla, P.L., and Singh, M.B. (2012a). Genomic profiling of rice sperm cell transcripts reveals conserved and distinct elements in the flowering plant male germ lineage. *New Phytol* 195, 560-573.**

Pubmed: [Author and Title](#)

CrossRef: [Author and Title](#)

Google Scholar: [Author Only Title Only Author and Title](#)

**Russell, S.D., Gou, X., Wong, C.E., Wang, X., Yuan, T., Wei, X., Bhalla, P.L., and Singh, M.B. (2012b). Genomic profiling of rice sperm cell transcripts reveals conserved and distinct elements in the flowering plant male germ lineage. *New Phytol* 195, 560-573.**

Pubmed: [Author and Title](#)

CrossRef: [Author and Title](#)

Google Scholar: [Author Only Title Only Author and Title](#)

**Sabelli, P.A., Hoerster, G., Lizarraga, L.E., Brown, S.W., Gordon-Kamm, W.J., and Larkins, B.A. (2009). Positive regulation of minichromosome maintenance gene expression, DNA replication, and cell transformation by a plant retinoblastoma gene. *Proc Natl Acad Sci USA* 106, 4042-4047.**

Pubmed: [Author and Title](#)

CrossRef: [Author and Title](#)

Google Scholar: [Author Only Title Only Author and Title](#)

**Sabelli, P.A., Liu, Y., Dante, R.A., Lizarraga, L.E., Nguyen, H.N., Brown, S.W., Klingler, J.P., Yu, J., LaBrant, E., Layton, T.M., Feldman, M., and Larkins, B.A. (2013). Control of cell proliferation, endoreduplication, cell size, and cell death by the retinoblastoma-related pathway in maize endosperm. *Proc Natl Acad Sci USA* 110, E1827-1836.**

Pubmed: [Author and Title](#)

CrossRef: [Author and Title](#)

Google Scholar: [Author Only Title Only Author and Title](#)

**Salvo, S.A.G.D., Hirsch, C.N., Buell, C.R., Kaeppler, S.M., and Kaeppler, H.F. (2014). Whole transcriptome profiling of maize during early somatic embryogenesis reveals altered expression of stress factors and embryogenesis-related genes. *PLoS ONE* 9, e111407.**

Pubmed: [Author and Title](#)

CrossRef: [Author and Title](#)

Google Scholar: [Author Only Title Only Author and Title](#)

**Sauter, M., von Wiegand, P., Lörz, H., and Kranz, E. (1998). Cell cycle regulatory genes from maize are differentially controlled during fertilization and first embryonic cell division. *Sex Plant Reprod* 11, 41-48.**

Pubmed: [Author and Title](#)

CrossRef: [Author and Title](#)

Google Scholar: [Author Only Title Only Author and Title](#)

**Schier, A.F. (2007). The maternal-zygotic transition: Death and birth of RNAs. *Science* 316, 406-407.**

Pubmed: [Author and Title](#)

CrossRef: [Author and Title](#)

Google Scholar: [Author Only Title Only Author and Title](#)

**Schnable, P.S., Ware, D., Fulton, R.S., Stein, J.C., Wei, F., Pasternak, S., Liang, C., Zhang, J., Fulton, L., Graves, T.A., Minx, P., Reily, A.D., Courtney, L., Kruchowski, S.S., Tomlinson, C., Strong, C., Delehaunty, K., Fronick, C., Courtney, B., Rock, S.M., Belter, E., Du, F., Kim, K., Abbott, R.M., Cotton, M., Levy, A., Marchetto, P., Ochoa, K., Jackson, S.M., Gillam, B., Chen, W., Yan, L., Higginbotham, J., Cardenas, M., Waligorski, J., Applebaum, E., Phelps, L., Falcone, J., Kanchi, K., Thane, T., Scimone, A., Thane, N., Henke, J., Wang, T., Ruppert, J., Shah, N., Rotter, K., Hodges, J., Ingenthron, E., Cordes, M., Kohlberg, S., Sgro, J., Delgado, B., Mead, K., Chinwalla, A., Leonard, S., Crouse, K., Collura, K., Kudrna, D., Currie, J., He, R., Angelova, A., Rajasekar, S., Mueller, T., Lomeli, R., Scara, G., Ko, A., Delaney, K., Wissotski, M., Lopez, G., Campos, D., Braidotti, M., Ashley, E., Golser, W., Kim, H., Lee, S., Lin, J., Dujmic, Z., Kim, W., Talag, J., Zuccolo, A., Fan, C., Sebastian, A., Kramer, M., Spiegel, L., Nascimento, L., Zutavern, T., Miller, B., Ambroise, C., Muller, S., Spooner, W., Narechania, A., Ren, L., Wei, S., Kumari, S., Faga, B., Levy, M.J., McMahan, L., Van Buren, P., Vaughn, M.W., Ying, K., Yeh, C.T., Enrich, S.J., Jia, Y., Kalyanaraman, A., Hsia, A.P., Barbazuk, W.B., Baucom, R.S., Brutnell, T.P., Carpita, N.C., Chaparro, C., Chia, J.M., Deragon, J.M., Estill, J.C., Fu, Y., Jeddalo, J.A., Han, Y., Lee, H., Li, P., Lisch, D.R., Liu, S., Liu, Z., Nagel, D.H., McCann, M.C., SanMiguel, P., Myers, A.M., Nettleton, D., Nguyen, J., Penning, B.W., Ponnala, L., Schneider, K.L., Schwartz, D.C., Sharma, A., Soderlund, C., Springer, N.M., Sun, Q., Wang, H., Waterman, M., Westerman, R., Wolfgruber, T.K., Yang, L., Yu, Y., Zhang, L., Zhou, S., Zhu, Q., Bennetzen, J.L., Dawe, R.K., Jiang, J., Jiang, N., Presting, G.G., Wessler, S.R., Aluru, S., Martienssen, R.A., Clifton, S.W., McCombie, W.R., Wing, R.A., and Wilson, R.K. (2009). The B73 maize genome: complexity, diversity, and dynamics. *Science* 326, 1112-1115.**

Pubmed: [Author and Title](#)

CrossRef: [Author and Title](#)

Google Scholar: [Author Only Title Only Author and Title](#)

**Schon, M.A., and Nodine, M.D. (2017). Widespread contamination of Arabidopsis embryo and endosperm transcriptome data sets. *Plant Cell* 29, 608-617.**

Pubmed: [Author and Title](#)

CrossRef: [Author and Title](#)

Google Scholar: [Author Only Title Only Author and Title](#)

**Schreiber, D.N., Bantin, J., and Dresselhaus, T. (2004). The MADS box transcription factor ZmMADS2 is required for anther and pollen maturation in maize and accumulates in apoptotic bodies during anther dehiscence. *Plant Physiol* 134, 1069-1079.**

Pubmed: [Author and Title](#)  
CrossRef: [Author and Title](#)  
Google Scholar: [Author Only Title Only Author and Title](#)

**Siller, K.H., and Doe, C.Q. (2009). Spindle orientation during asymmetric cell division. *Nat Cell Biol* 11, 365-374.**

Pubmed: [Author and Title](#)  
CrossRef: [Author and Title](#)  
Google Scholar: [Author Only Title Only Author and Title](#)

**Thomas, J.O., and Travers, AA (2001). HMG1 and 2, and related 'architectural' DNA-binding proteins. *Trends Biochem Sci* 26, 167-174.**

Pubmed: [Author and Title](#)  
CrossRef: [Author and Title](#)  
Google Scholar: [Author Only Title Only Author and Title](#)

**Tuteja, N., Tran, N., Dang, H., and Tuteja, R. (2011). Plant MCM proteins: role in DNA replication and beyond. *Plant Mol Biol* 77, 537-545.**

Pubmed: [Author and Title](#)  
CrossRef: [Author and Title](#)  
Google Scholar: [Author Only Title Only Author and Title](#)

**Uebler, S., Márton, M.L., and Dresselhaus, T. (2015). Classification of EA1-box proteins and new insights into their role during reproduction in grasses. *Plant Reprod* 28, 183-197.**

Pubmed: [Author and Title](#)  
CrossRef: [Author and Title](#)  
Google Scholar: [Author Only Title Only Author and Title](#)

**Vandepoele, K., Raes, J., Veylder, L., Rouzé, P., Rombauts, S., and Inzé, D. (2002). Genome-wide analysis of core cell cycle genes in *Arabidopsis*. *Plant Cell* 14, 903-916.**

Pubmed: [Author and Title](#)  
CrossRef: [Author and Title](#)  
Google Scholar: [Author Only Title Only Author and Title](#)

**Vilella, A.J., Severin, J., Ureta-Vidal, A., Heng, L., Durbin, R., and Birney, E. (2009). EnsemblCompara GeneTrees: Complete, duplication-aware phylogenetic trees in vertebrates. *Genome Res* 19, 327-335.**

Pubmed: [Author and Title](#)  
CrossRef: [Author and Title](#)  
Google Scholar: [Author Only Title Only Author and Title](#)

**Wagner, G.P., Kin, K., and Lynch, V.J. (2012). Measurement of mRNA abundance using RNA-seq data: RPKM measure is inconsistent among samples. *Theory Biosci* 131, 281-285.**

Pubmed: [Author and Title](#)  
CrossRef: [Author and Title](#)  
Google Scholar: [Author Only Title Only Author and Title](#)

**Wei, K., Chen, J., Wang, Y., Chen, Y., Chen, S., Lin, Y., Pan, S., Zhong, X., and Xie, D. (2012). Genome-wide analysis of bZIP-encoding genes in maize. *DNA Res* 19, 463-476.**

Pubmed: [Author and Title](#)  
CrossRef: [Author and Title](#)  
Google Scholar: [Author Only Title Only Author and Title](#)

**Wu, R.-C., Jiang, M., Beaudet, A.L., and Wu, M.-Y. (2013). ARID4A and ARID4B regulate male fertility, a functional link to the AR and RB pathways. *Proc Natl Acad Sci USA* 110, 4616-4621.**

Pubmed: [Author and Title](#)  
CrossRef: [Author and Title](#)  
Google Scholar: [Author Only Title Only Author and Title](#)

**Wuest, S.E., Vijverberg, K., Schmidt, A., Weiss, M., Gheyselinck, J., Lohr, M., Wellmer, F., Rahnenfuhrer, J., von Mering, C., and Grossniklaus, U. (2010). *Arabidopsis* female gametophyte gene expression map reveals similarities between plant and animal gametes. *Curr Biol* 20, 506-512.**

Pubmed: [Author and Title](#)  
CrossRef: [Author and Title](#)  
Google Scholar: [Author Only Title Only Author and Title](#)

**Yue, R., Tie, S., Sun, T., Zhang, L., Yang, Y., Qi, J., Yan, S., Han, X., Wang, H., and Shen, C. (2015). Genome-wide identification and expression profiling analysis of ZmPIN, ZmPILS, ZmLAX and ZmABCB auxin transporter gene families in maize (*Zea mays* L.) under various abiotic stresses. *PLoS One* 10, e0118751.**

Pubmed: [Author and Title](#)  
CrossRef: [Author and Title](#)  
Google Scholar: [Author Only Title Only Author and Title](#)

**Zhang, Z., Li, X., Han, M., and Wu, Z. (2015). Genome-wide analysis and functional identification of the annexin gene family in maize (*Zea mays* L.). *Plant Omics* 8, 420-428.**

Pubmed: [Author and Title](#)  
CrossRef: [Author and Title](#)  
Google Scholar: [Author Only Title Only Author and Title](#)

**Zhao, P., and Sun, M.X. (2015). The maternal-to-zygotic transition in higher plants: Available approaches, critical limitations, and**

**technical requirements.** *Curr Top Dev Biol* 113, 373-398.

Pubmed: [Author and Title](#)

CrossRef: [Author and Title](#)

Google Scholar: [Author Only](#) [Title Only](#) [Author and Title](#)

**Zhao, P., Begcy, K., Dresselhaus, T., and Sun, M.X. (2017).** Does early embryogenesis in eudicots and monocots involve the same mechanism and molecular players? *Plant Physiol* 173, 130-142.

Pubmed: [Author and Title](#)

CrossRef: [Author and Title](#)

Google Scholar: [Author Only](#) [Title Only](#) [Author and Title](#)

**Zheng, B., He, H., Zheng, Y., Wu, W., and McCormick, S. (2014).** An ARID domain-containing protein within nuclear bodies is required for sperm cell formation in *Arabidopsis thaliana*. *PLoS Genet* 10, e1004421.

Pubmed: [Author and Title](#)

CrossRef: [Author and Title](#)

Google Scholar: [Author Only](#) [Title Only](#) [Author and Title](#)

**Zhou, D.X., Bisanz-Seyer, C., and MacHe, R. (1995).** Molecular cloning of a small DNA binding protein with specificity for a tissue-specific negative element within the *rps1* promoter. *Nucl Acids Res* 23, 1165-1169.

Pubmed: [Author and Title](#)

CrossRef: [Author and Title](#)

Google Scholar: [Author Only](#) [Title Only](#) [Author and Title](#)

**Zygotic Genome Activation Occurs Shortly After Fertilization in Maize**  
Junyi Chen, Nicholas Strieder, Nadia G. Krohn, Philippe Cyprys, Stefanie Sprunck, Julia C.  
Engelmann and Thomas Dresselhaus  
*Plant Cell*; originally published online August 16, 2017;  
DOI 10.1105/tpc.17.00099

This information is current as of August 29, 2017

<b>Supplemental Data</b>	<a href="/content/suppl/2017/08/16/tpc.17.00099.DC1.html">/content/suppl/2017/08/16/tpc.17.00099.DC1.html</a>
<b>Permissions</b>	<a href="https://www.copyright.com/ccc/openurl.do?sid=pd_hw1532298X&amp;issn=1532298X&amp;WT.mc_id=pd_hw1532298X">https://www.copyright.com/ccc/openurl.do?sid=pd_hw1532298X&amp;issn=1532298X&amp;WT.mc_id=pd_hw1532298X</a>
<b>eTOCs</b>	Sign up for eTOCs at: <a href="http://www.plantcell.org/cgi/alerts/ctmain">http://www.plantcell.org/cgi/alerts/ctmain</a>
<b>CiteTrack Alerts</b>	Sign up for CiteTrack Alerts at: <a href="http://www.plantcell.org/cgi/alerts/ctmain">http://www.plantcell.org/cgi/alerts/ctmain</a>
<b>Subscription Information</b>	Subscription Information for <i>The Plant Cell</i> and <i>Plant Physiology</i> is available at: <a href="http://www.aspb.org/publications/subscriptions.cfm">http://www.aspb.org/publications/subscriptions.cfm</a>